PERGAMON Computers and Mathematics with Applications 43 (2002) 551–583

An International Journal
computers & mathematics
with applications

www.elsevier.com/locate/camwa

A Comparison Analysis between Unsymmetric and Symmetric Radial Basis Function Collocation Methods for the Numerical Solution of Partial Differential Equations

H. POWER
Department of Mechanical Engineering
The University of Nottingham
University Park, Nottingham, NG7 2RD, U.K.

V. BARRACO
Wessex Institute of Technology, Ashurst Lodge
Ashurst, Southampton SO40 7AA, U.K.
and
Universita Degli Studi di Palermo
Facolta di Ingegneria, Ingegneria Aeronautica, Palermo, Italy

Abstract—In this article, we present a thorough numerical comparison between unsymmetric and symmetric radial basis function collocation methods for the numerical solution of boundary value problems for partial differential equations. A series of test examples was solved with these two schemes, different problems with different type of governing equations, and boundary conditions. Particular emphasis was paid to the ability of these schemes to solve the steady-state convection-diffusion equation at high values of the Péclet number. From the examples tested in this work, it was observed that the system of algebraic equations obtained with the symmetric method was in general simpler to solve than the one obtained with the unsymmetric method and that the resulting algorithm performs better. However, the unsymmetric method has the advantage of being simpler to implement. Two main features about the results obtained in this work are worthy of special attention: First, with the symmetric method it was possible to solve convection-diffusion problems at a very high Péclet number without the need of any artificial damping term, and second, with these two approaches, symmetric and unsymmetric, it is possible to impose free boundary conditions for problems in unbounded domains.

Keywords—Partial differential equation, Numerical solution, Mesh free technique.

1. INTRODUCTION

In recent years, the theory of radial basis functions (RBFs) has undergone intensive research and enjoyed considerable success as a technique for interpolating multivariable data and functions. Unlike other interpolating functions, RBFs are not restricted to problems with only convex hulls or uniform data spacing.

A radial basis function, $\Psi(\mathbf{x} - \mathbf{x}_j) = \psi(\|\mathbf{x} - \mathbf{x}_j\|)$, is a continuous spline which depends upon the separation distances of a subset of data centres, $X \subset \Re^n$, $\{\mathbf{x}_j \in X,\ j = 1, 2, \ldots, N\}$. Due

0898-1221/02/$ - see front matter Typeset by AMS-TEX
PII: S0898-1221(01)00305-4

to RBFs' spherical symmetry about the centres $\mathbf{x}_j$ (nodal or collocation points), they are called radial. The distances, $\|\mathbf{x} - \mathbf{x}_j\|$, are usually taken to be the Euclidean metric, although other metrics are possible (for more details, see [1]).

The most popular RBFs are

$$r^{2m-2} \log r \text{ (generalized thin plate splines)},$$
$$\left(r^2 + c^2\right)^{m/2} \text{ (generalized multiquadric)},$$
$$e^{-\beta r} \text{ (Gaussian)},$$

where m is an integer number and $r = \|\mathbf{x} - \mathbf{x_j}\|$.

The Gaussian and the inverse multiquadric, i.e., $m < 0$ in the generalized multiquadric function, are positive definite functions, while the thin-plate splines and the multiquadric, i.e., $m > 0$ in the generalized multiquadric function, are conditionally positive definite functions of order m, which require the addition of a polynomial term P of order $m - 1$ together with some homogeneous constraint conditions in order to obtain an invertible interpolation matrix. The multiquadric functions with values of $m = 1$ and $c = 0$ are often referred to as conical functions whilst with $m = 3$ and $c = 0$ as Duchon cubics.

In a typical problem, we have N pairs of data points $\{(\mathbf{x}_j, F(\mathbf{x}_j))_{j=1}^N\}$, which are assumed to be samples of some unknown function F that is to be interpolated by the function f, i.e.,

$$f(\mathbf{x}) = \sum_{j=1}^{N} \lambda_j \Psi\left(\|\mathbf{x} - \mathbf{x_j}\|\right) + P_m(\mathbf{x}), \qquad \mathbf{x} \in \Re^2, \tag{1}$$

in the sense that

$$F\left(\mathbf{x_i}\right) = \sum_{j=1}^{N} \lambda_j \Psi\left(\|\mathbf{x_i} - \mathbf{x_j}\|\right) + P_m\left(\mathbf{x_i}\right), \tag{2}$$

along with the constrains

$$\sum_{j=1}^{N} \lambda_j P_k\left(\mathbf{x_j}\right) = 0, \qquad 1 \le k \le m. \tag{3}$$

Here the numbers λ_j, $j = 1, 2, \ldots, N$, are real coefficients and Ψ is a radial basis function.

The matrix formulation of the above interpolation problem can be written as $\mathbf{Ax} = \mathbf{b}$ with

$$A = \begin{pmatrix} \Psi & P_m \\ P_m^{\top} & 0 \end{pmatrix}, \tag{4}$$

$\mathbf{x}^{\top} = (\boldsymbol{\lambda}, \boldsymbol{\beta})$ and $\mathbf{b}^{\top} = (\mathbf{F}, \mathbf{0})$, where β are the coefficients of the polynomial.

Micchelli [2] proved that for a case when the nodal points are all distinct, the matrix resulting from the above radial basis function interpolation is always nonsingular. Numerical experiments show that the condition number of the above interpolation matrix for smooth RBFs like Gaussian or multiquadrics are extremely large when compared with those resulting from nonsmooth RBFs like the thin-plate splines (see [3]). Moreover, in the literature of RBF interpolation with the functions given above, there is no known case where the error and the sensitivity are both reasonably small (uncertainty principle), which means that good convergence can only be achieved at the expense of instability.

In 1982, Franke [4] published a review article evaluating virtually all the interpolation methods for scattered data sets available at that time. Among the methods tested, RBFs outperformed all the other methods regarding accuracy, stability, efficiency, memory requirement, and simplicity of implementation. In a similar study, Stead [5] examined the accuracy of partial derivative approximations over scattered data sets, also concluding that RBFs performed more accurately

compared to other considered methods. Of the RBFs tested by Franke, Hardy's multiquadrics (MQ) were ranked the best in accuracy, followed by Duchon's thin plate splines (TPS), i.e., the generalized multiquadric and thin plate splines with $m = 1$ and $m = 2$, respectively.

Duchon [6] derived the TPS as an optimum solution to the interpolation problem in a certain Hilbert space via construction of a reproducing kernel. Therefore, they are the natural generalization of cubic splines in $n > 1$ dimension. Even though TPS have been considered as optimal interpolating multivariate functions, they do, however, only converge linearly (see [7]). On the other hand, the MQ functions converge exponentially and always produce a minimal seminorm error as proved by Madych and Nelson [8]. However, despite MQ's excellent performance, it contains a free parameter, c^2, often referred to as the shape parameter. When c is small, the resulting interpolating surface is pulled tightly to the data points, forming a cone-like basis functions. As c increases, the peak of the cone gradually flattens.

The choice of the value of c can greatly affect the accuracy of the approximation. Tarwater [9] found that by increasing c, the root-mean-square error of the goodness-of-fit dropped to a minimum value and then grew rapidly thereafter. In general, when c becomes large, $c^2 \gg r^2$, the MQ coefficient matrix becomes ill-conditioned and the condition number becomes an important factor in choosing the shape parameter.

How to choose the optimal shape parameter is a problem that has received the attention of many researchers. Early works recommended the choice of the value of c to be proportional to the mean distance from each data point to its nearest neighbour. Franke [10] used the formula

$$c^2 = (1.25)^2 d^2, \tag{5}$$

where d is the mean distance. Carlson and Foley [11] showed that the behaviour of the function to be interpolated has an important role in determining the optimal value of the shape parameter. They suggested that a small value of c be used if the function varies rapidly, but a large value be used if the function has large curvature (smooth function). Following this idea, Kansa [12] suggested a variable shape parameter and observed that with the use of variable c_j^2, the resulting matrix lost its symmetric property, but its condition number reduced significantly.

So far, the choice of the optimal value of the shape parameter remains an open problem; no mathematical theory has been yet developed to determine such optimal value. Similar difficulties are encountered in choosing the shape parameter for the inverse multiquadric functions.

In general, the mathematical description of physical processes leads to partial differential equations (PDEs). In most cases, the solution of such problems needs to be found by numerical analysis. The equations can be solved using finite difference (FDM), finite element (FEM), finite volume (FVM), and boundary elements (BEM) methods. These methods require the definition of a mesh (domain discretization) where the functions are approximated locally. The construction of a mesh in two or more dimensions is a nontrivial problem. Usually, in practice, only low-order approximations are employed (none Hermitian) resulting in a continuous approximation of the function across the mesh but not its partial derivatives. The discontinuity of the approximation of the derivative can adversely affect the stability of the solution. While higher-order schemes are necessary for more accurate approximations of the spatial derivatives, they usually involve additional computational cost. To increase the accuracy of low-order schemes, it is required that the computational mesh be refined with a higher density of elements in the regions near the contours. This, however, is also achieved at the expense of increased computational cost.

Although most work to date on RBFs relates to scattered data approximation and in general to interpolation theory, there has recently been an increased interest in their use for solving PDEs. This approach, which approximates the whole solution of the PDE directly using RBFs, is very attractive due to the fact that this is truly a mesh-free technique. Kansa [13] introduced the concept of solving PDEs using RBFs. Considering Franke's results, he focused upon the MQ function and argued that PDEs are intrinsically related to the interpolation scheme from which PDE solvers are derived.

More recently, Fasshauer [14] suggested an alternative approach based on the Hermite interpolation property of the radial basis functions, which states that the RBFs not only are able to interpolate a given function, but also its derivatives. The convergence proof for RBF Hermite-Birkhoff interpolation was given by Wu [15] who also recently proved the convergence of this approach when solving PDEs [16]; see also [17].

For a boundary value problem

$$L[u](\mathbf{x}) = f(\mathbf{x}), \qquad \mathbf{x} \in \Omega, \tag{6}$$

$$B[u](\mathbf{x}) = g(\mathbf{x}), \qquad \mathbf{x} \in \Gamma, \tag{7}$$

where the operators L and B are linear partial differential operators on the domain Ω and at the contour Γ, respectively. An unsymmetric RBF collocation method, as is the case of Kansa's method, represents the solution u by the interpolation (1), where the N data points, $\mathbf{x}_j$, $j = 1, 2, \ldots N$, are divided into a set of n boundary points and $N - n$ interior points, i.e.,

$$u(\mathbf{x}) = \sum_{j=1}^{N} \lambda_j \Psi \left(\|\mathbf{x} - \boldsymbol{\xi}_j\| \right) + P_m(\mathbf{x}). \tag{8}$$

At the interior points, it is required that the partial differential equation (6) be satisfied while the boundary condition, i.e., equation (7), is imposed at the boundary points, with additional constraint conditions

$$\sum_{j=1}^{N} \lambda_j P_k \left(\mathbf{x_i} \right) = 0, \qquad 1 \leq k \leq m.$$

In this way, a linear system of algebraic equations is found for the coefficients λ_j, $j = 1, 2, \ldots N$, and the polynomial coefficients, whose collocation matrix is

$$A = \begin{pmatrix} B_{\mathbf{x}}[\Psi] & B_{\mathbf{x}}[P_m] \\ L_{\mathbf{x}}[\Psi] & L_{\mathbf{x}}[P_m] \\ P_m^{\mathsf{T}} & 0 \end{pmatrix}, \tag{9}$$

where the partial derivatives in the operators L and B are taken with respect to the variable $\mathbf{x}$. Although the above approach has been applied successfully in several cases (see, for example, [18–22]), no existence of solution and convergence analysis is available in the literature and, for some cases, it has been reported that the resulting matrix was extremely ill-conditioned and even singular for some distribution of the nodal points (see [23]).

It is important to observe that for conditionally positive definite functions such as the TPS and the MQ, the addition of the polynomial term is necessary to guarantee the existence of the inverse of the interpolation matrix (4). However, it is not clear what role the polynomial term plays on the solution of partial differential equations with unsymmetric collocation RBF methods, since there is no available proof of the existence of the inverse of the unstructured matrix (9).

Kansa's method is an unsymmetric RBF collocation method based upon the MQ interpolation functions, in which the shape parameter is considered to be variable across the problem domain. The distribution of the shape parameter is obtained by an optimization approach, in which the value of c_j^2 is assumed to be proportional to the curvature of the unknown solution of the original partial differential equation. In this way, it is possible to reduce the condition number of the matrix (9) at the expense of implementing an additional iterative algorithm. In the present work, we will implement the unsymmetric collocation method in its simpler form, without any optimization of the interpolation functions and the collocation points.

On the other hand, for a symmetric RBF collocation method, as is the case of Fasshauer's method, the solution of the boundary value problem is approximated by

$$u(\mathbf{x}) = \sum_{k=1}^{n} \lambda_k \bar{B}_{\xi} \Psi \left(\|\mathbf{x} - \boldsymbol{\xi}_k\| \right) + \sum_{k=n+1}^{N} \lambda_k \bar{L}_{\xi} \Psi \left(\|\mathbf{x} - \boldsymbol{\xi}_k\| \right) + P_m(\mathbf{x}),$$

where n denotes the number of nodes on the boundary of Ω, and $\bar{L}_{\boldsymbol{\xi}}$ and $\bar{B}_{\boldsymbol{\xi}}$ are the adjoint differential operators of those used in (6) and (7), but acting on Ψ viewed as a function of the second argument $\boldsymbol{\xi}$. This form of the operators is chosen in order to guarantee symmetry.

This expansion for u leads to a collocation matrix A which is of the form

$$\mathbf{A} = \begin{pmatrix} B_{\mathbf{x}}\bar{B}_{\boldsymbol{\xi}}[\Psi] & B_{\mathbf{x}}\bar{L}_{\boldsymbol{\xi}}[\Psi] & B_{\mathbf{x}}P_m \\ L_{\mathbf{x}}\bar{B}_{\boldsymbol{\xi}}[\Psi] & L_{\mathbf{x}}\bar{L}_{\boldsymbol{\xi}}[\Psi] & L_{\mathbf{x}}P_m \\ B_{\mathbf{x}}P_m^{\mathsf{T}} & L_{\mathbf{x}}P_m^{\mathsf{T}} & 0 \end{pmatrix}. \tag{10}$$

The matrix (10) is of the same type as the scattered Hermite interpolation matrices, and thus nonsingular as long as Ψ is chosen appropriately. The convergence of the above approach has been proven by Schaback and Franke [17] in terms of a generalized Fourier transform analysis (see also [16]). Another point in favour of the Hermite-based approach is that the matrix (10) is symmetric, as opposed to the completely unstructured matrix (9) of the same size.

In contrast to the unstructured matrix (9), unsymmetric approach, in the case of the Hermite interpolation matrix (10), symmetric approach, it is possible to prove that for conditionally positive definite functions like the TPS and the MQ, it is necessary to add a polynomial term in order to guarantee the existence of the inverse of the matrix (for more details, see [15]).

As in the case of the unsymmetric approach, in order to be consistent and keep the formulation simpler, in our implementation of the symmetric approach, no optimization of the interpolation functions and the collocation points will be considered.

From a series of simple numerical examples, Fasshauer concluded that it seems that the symmetric method performs slightly better than the unsymmetric one. In this work, we will present a thorough numerical comparison between these two schemes for different problems, with different types of governing equations and different boundary conditions.

Due to the uncertainty regarding which RBF is the best to use in a collocation method for the solution of boundary value problems for partial differential equations, in this work we will use the two most popular functions, namely, the TPS and the MQ. Even for standard multivariable data interpolation, it is not clear which RBF will produce the best results with less computational cost, as can be concluded from the previous literature survey. A possible alternative is the use of the positive definite Wendland [24] compactly supported radial basis functions, but as pointed out by Schaback and Wendland [25], the choice of the support and the smoothness of such functions seems to require some numerical experience.

From the examples tested here, it was observed that the system of algebraic equations obtained with the symmetric method was in general simpler to solve than the one obtained with the unsymmetric method, and that the resulting algorithm performs better. However, the unsymmetric method has the advantage of being simpler to implement.

2. NUMERICAL ANALYSIS

In this section, we present the numerical results for different boundary value problems obtained with each of the above two mesh-free methods and a comparison between their solutions.

2.1. Unsymmetric Method

As pointed out in the Introduction, it is not clear which role plays the polynomial term in the solution of the unstructured matrix (9) resulting from the application of an unsymmetric RBF collocation method. For this reason, in this section we will test the behaviour of the system of equations defined by (8) and (9), which represents an approximate solution of the boundary value problem (6) and (7), in terms of the thin plate splines and multiquadric functions with and without the polynomial term.

2.1.1. Laplace's equation

In this case, it is required that we use at least a generalized thin plate spline function of the order $m = 3$, TPS^3, in order to avoid the singularity at $r = 0$ appearing from the Laplacian operator in the matrix (9).

(I) Dirichlet boundary condition in a rectangular domain

Let us consider the solution of the Laplace equation in a rectangular domain $[1 \times 0.6]$, with the following boundary conditions:

$$\begin{aligned} &\phi = 0, && 0 \le x \le 1, && y = 0 \\ &\phi = f(x), && 0 \le x \le 1, && y = 0.6 \\ &\phi = 0, && 0 \le y \le 0.6, && x = 0 \\ &\phi = 0, && 0 \le y \le 0.6, && x = 1. \end{aligned} \tag{11}$$

The analytical solution of the above problem is given by

$$\Phi(x, y) = \sum_{n=1}^{\infty} c_n \sin\left(\frac{n\pi x}{l}\right) \frac{\sinh(n\pi y/l)}{\sinh(n\pi\, d/l)}, \tag{12}$$

where

$$c_n = \frac{2}{l} \int_0^l f(x) \sin\left(\frac{n\pi x}{l}\right) dx$$

and l and d are the dimensions of the rectangular.

In our case, $l = 1$, $d = 0.6$, and the function f is defined as a triangular function

$$f(x) = \begin{cases} 2x, & 0 \le x \le 0.5, \\ 2 - 2x, & 0.5 \le x \le 1. \end{cases} \tag{13}$$

As a first example, we solved the above case using the MQ function without the polynomial term as the interpolating function, with a shape parameter $c = 1$. The resulting algebraic system of equations was solved using Gauss elimination. Figure 1 shows the relative error between the analytical and the numerical solutions when we used 77 uniformly distributed collocation points, of which 32 were boundary points and the remaining 45 internal points (see Figure 2). The local relative error, i.e., $(\phi_t - \phi_n)/\phi_t$ with ϕ_t and ϕ_n as the analytical and numerical values, respectively, was evaluated at the internal points where the partial differential equation was imposed and not the boundary conditions. Using the above configuration of collocation points, the maximum relative error was 4.2% on the line $y = 0.1$, and near the vertical walls, when we added the polynomial term, no improvement was observed. Using the TPS^3 function without the polynomial term, instead of the MQ function, the maximum relative error increased to a value of 6.8%; however, when the polynomial term was introduced, we found an accuracy similar to the one obtained with the MQ. In this case, the maximum relative error is again found near the lower boundary with a value of 4.9%.

In order to improve the accuracy, we increased the number of collocation points. Using 273 collocation points uniformly distributed, 64 on the boundary and 209 inside the domain, and employing the MQ function with $c = 1$ and without the polynomial term, the maximum relative error was further reduced to 3.2% near the boundaries where the value of the potential was prescribed equal to zero; it, however, rapidly decreased to a value around 0.45% in the middle regions (Figure 3). As before, no improvement was obtained by adding the polynomial. The accuracy was also improved when using the TPS^3 function with the polynomial term, resulting in a maximum relative error of 0.9%. From the previous results, we can observe that the bigger relative errors were always near to the boundaries.

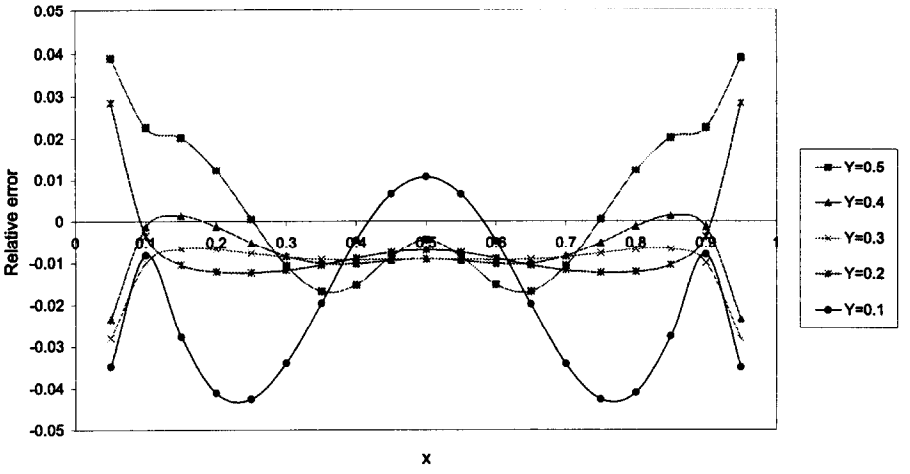

Figure 1. Relative error obtained with the unsymmetric method based on the MQ function with the distribution of 77 collocation points.

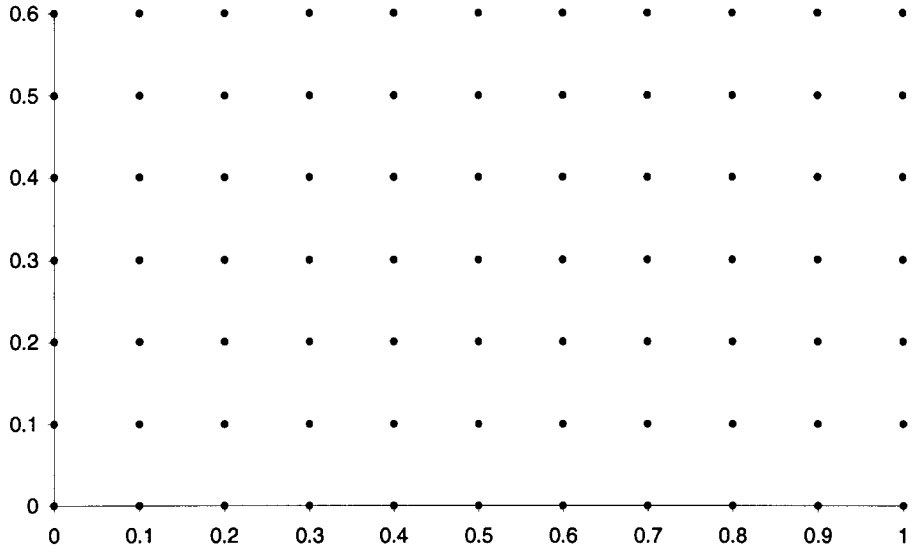

Figure 2. Uniform distribution of 77 collocation points.

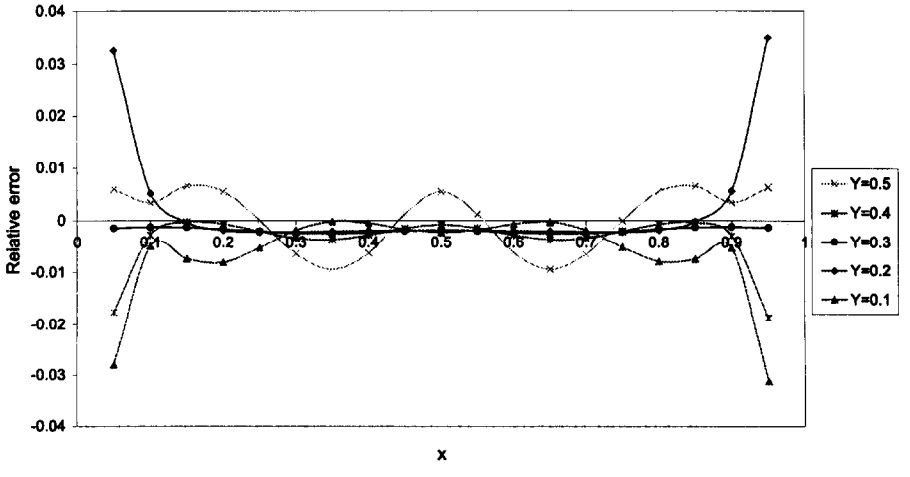

Figure 3. Relative error obtained with the unsymmetric method based on the MQ function with the distribution of 273 collocation points.

The relative error at the boundary, which was measured at the middle point between the boundary collocation points, was always of the same order of magnitude as those at the core region of the interior points. A maximum value of 0.38%, found at the line $y = 0$, was obtained in the case of 273 collocation points.

Similar results to the one obtained here have been previously reported in the literature (see [26]), where typically the largest error was found near the boundary with a magnitude of one or two order larger than those in the domain far from the boundary. In order to improve this difference in accuracy, Fedoseyev *et al.* [26] proposed the use of a set of additional boundary nodes, different to the one used to impose the boundary conditions, where the partial differential equation is imposed. With this modification, they observed that the relative error near the boundary was dramatically reduced.

It is important to point out that the above results obtained with the MQ function can be improved by choosing an appropriate value of the parameter c. In the next example, we will discuss this alternative.

To see if it is possible to improve the accuracy of the results near the boundaries, by using different node distributions, we solved the above problem using several nonuniform distributions of nodes and even a random distribution of internal nodes. However, no major improvement was observed.

(II) Circular domain

We will now solve the Laplace equation in a circle domain for different types of boundary conditions and using different interpolation functions. Moreover, we will estimate the normal derivative on the boundary after finding the solution of a Dirichlet boundary value problem.

A general regular solution in a bounded domain of the Laplace equation in polar coordinates can be given in terms of the following linear combination of internal cylindrical harmonic functions:

$$\Phi(\mathbf{x}) = \sum_{i=0}^{\infty} A_{m_i} r^{m_i} \cos(m_i \vartheta) + \sum_{i=0}^{\infty} B_{n_i} r^{n_i} \sin(n_i \vartheta)$$

for any arbitrary constants A_{m_i} and B_{n_i}; here r is the distance between the point $\mathbf{x} = (x, y)$ and the origin of the Cartesian axis, and ϑ is the angle that the vector $\mathbf{r}$ forms with the x-axis, i.e., $r = \sqrt{x^2 + y^2}$ and $\vartheta = \arctan y/x$. For our example, we chose $A_3 = 2$, $B_4 = 5$, and all the other constants equal to zero, i.e.,

$$\Phi(\mathbf{x}) = 2r^3 \cos(3\vartheta) + 5r^4 \sin(4\vartheta). \tag{14}$$

For a unit radius circle located at the point $(1, 1)$, the components of the normal vector $\mathbf{n}$ are: $n_x = x - 1$ and $n_y = y - 1$, where x and y are the coordinates of a point on the boundary. The normal derivative of the above potential at the contour of such unit circle is

$$\begin{aligned} \left.\frac{\partial \Phi}{\partial n}\right|_{\Gamma} &= \frac{\partial \Phi}{\partial x} n_x + \frac{\partial \Phi}{\partial y} n_y = 6r^3 \cos(3\vartheta) + 20r^4 \sin(4\vartheta) \\ &+ 6r^2(\sin(2\vartheta) - \cos(2\vartheta)) - 20r^3(\sin(3\vartheta) + \cos(3\vartheta)). \end{aligned} \tag{15}$$

For simplicity, we calculated the relative error between the analytical and the numerical solutions at the internal points on the main diagonal $y = 1$ of the circle. Figure 4 shows the values of the potential given by the above analytical solution on this line. In our examples we used 361 uniformly distributed collocation points, of which 56 are at the boundary and 305 inside the domain (Figure 5).

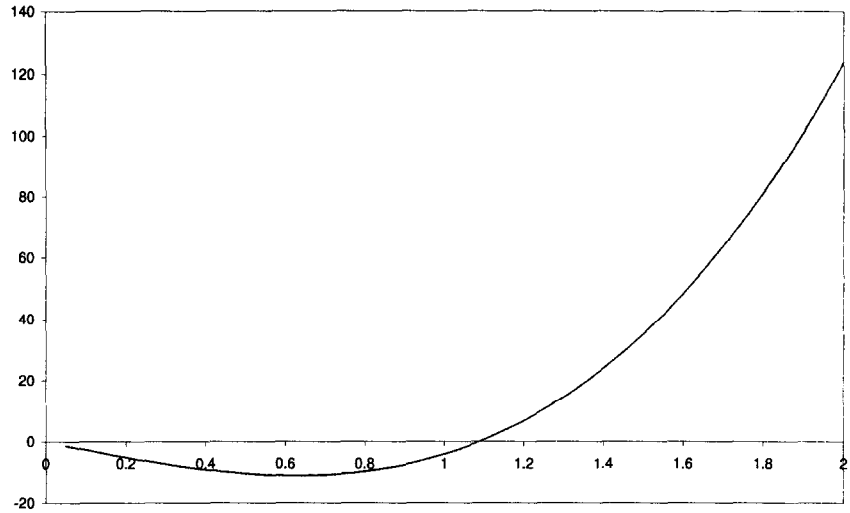

Figure 4. Analytical values of the potential on the line $y = 1$ for a circle centre at the point $(1, 1)$.

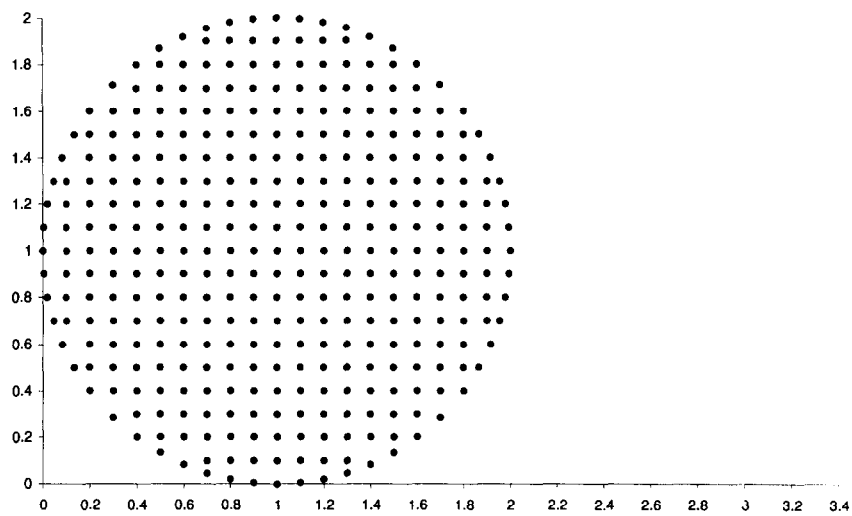

Figure 5. Distribution of 361 collocation points.

Dirichlet boundary condition

In our analysis, we first used the MQ function. In this case, we tested different values of the shape parameter c. As pointed out before, the performance of a multivariable data interpolation with the use of the multiquadric functions is significantly affected by the value of the shape parameter c. In the past, there have been several numerical experiments and empirical formulae that suggest how to choose the optimal value of such parameters, which in general depend on the density of the interpolation points' centres; see equation (5). However, it is not clear if these previous experiences with multivariable interpolation are still valid when the multiquadric functions are used in a collocation method to solve partial differential equations. In Tables 1 and 2, we report the optimal value of the shape parameter suggested by Fasshauer [14] for two different RBF collocation methods, unsymmetric and symmetric, for the numerical solution of the Poisson equation with two different nonhomogeneous terms and for different uniform distribution of collocations points, as well as the value of c predicted by equation (5), which was suggested by Franke [10] to obtain the optimal value of the shape parameter for a multivariable data interpolation. As can be observed, there is not a direct relation between the values of the

Table 1. Values of the shape parameter for Fasshauer's first Poisson problem.

Collocation Points	c Unsymmetric	c Symmetric	c Franke
15	1.18	1.39	0.636
24	1.04	1.11	0.339
60	4.80	3.84	0.198
128	3.12	3.12	0.085
240	2.00	2.30	0.050

Table 2. Values of the shape parameter for Fasshauer's second Poisson problem.

Collocation Points	c Unsymmetric	c Symmetric	c Franke
25	1.80	1.73	0.404
49	1.58	3.56	0.206
100	2.80	3.29	0.101
196	2.28	2.62	0.052
400	1.53	1.91	0.025

parameter c recommended for multivariable interpolation and those required by the collocation methods; even more, each collocation method requires different values of c.

Due to the uncertainty of how to choose the optimal value of c when an RBF collocation method is used in terms of the multiquadric functions, in this work we do not pretend to obtain the optimal value of such parameter, but instead we carried out a sensitivity analysis of the solutions for different values of c, ranging from 0.5 to 10 with an increment of one from one to ten. Instead of looking for the optimal value of c, we will test how the unsymmetric and symmetric collocation methods behave when they are based upon the thin plate spline functions, which do not have the problem of an adjustable parameter.

From the harmonic potential given by equation (14), we can define the Dirichlet boundary condition over the circle $(x-1)^2+(y-1)^2=1$. When the resulting system of linear algebraic equations was solved by Gauss elimination, the best result was found with a value of $c=1$, yielding a maximum relative error of 0.044% (Figure 6). We also tested the behaviour of the algorithm when using different solvers. Using a GMRES iterative solver, the best result was obtained with the value of the shape parameter equal to two instead of one, yielding a maximum relative error of 0.01% (Figure 7). No significant improvements were observed by adding the polynomial term to the MQ, but, in this case, the best value of the shape parameter was two for both the Gauss and the GMRES solvers.

Using the TPS^3, we did not improve the accuracy. The maximum relative error was 5.7% near the point $x=0$, but less than 0.45% from the point $x=0.2$ up to the point $x=2$. With the use of the TPS^3, both solvers, Gauss and GMRES, gave the same results (Figure 8). By adding the polynomial term, we found some small improvement, a maximum relative error of 3.6% instead of the 5.7% obtained without the polynomial term.

When the values of the function to be predicted are larger in magnitude than the one corresponding to the circle centre at the point $(1,1)$, as is the case when the circle is centered at the point $(3,3)$ (see Figure 9), the error of the numerical results reduced significantly, as can be observed in Figure 10. The best result with the MQ was obtained with $c=2$, yielding a maximum relative error of $4\cdot 10^{-4}\%$ and 0.05% when the TPS^3 was used.

Normal derivative of a Dirichlet problem

With the obtained solution of the above Dirichlet boundary value problem, we estimated the normal derivative of the potential over the perimeter of the circle. As before, the best results

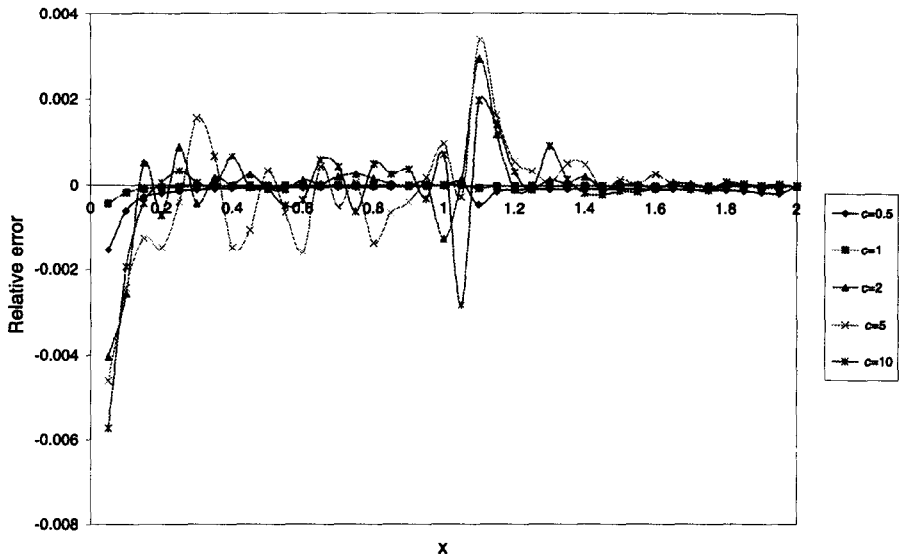

Figure 6. Relative error on the Dirichlet problem obtained with the unsymmetric method based on the MQ function and solved with the Gauss solver.

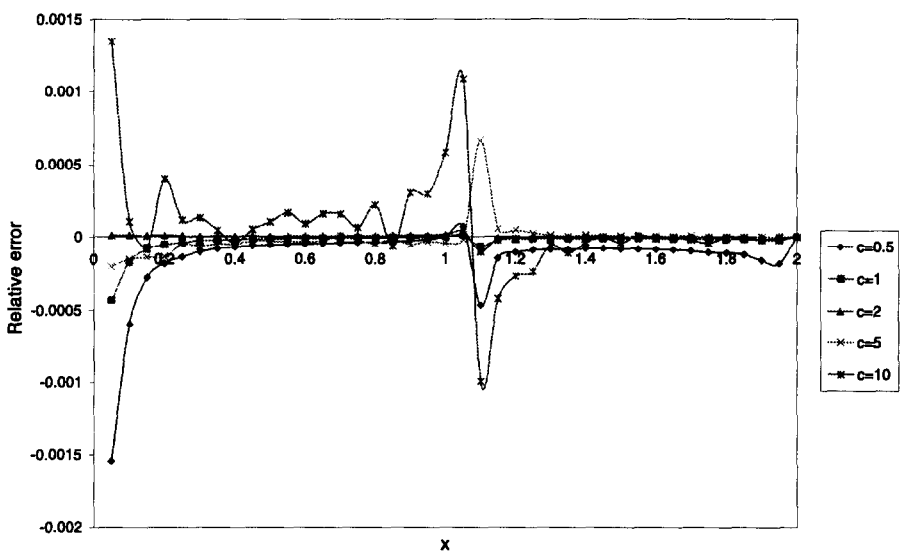

Figure 7. Relative error on the Dirichlet problem obtained with the unsymmetric method based on the MQ function and solved with the GMRES iterative solver.

were obtained with different values of the shape parameter according to the type of solver used. Using the MQ function and the Gauss solver, a maximum relative error of 0.12% (Figure 11) was found when the value of the shape parameter was equal to one. The GMRES gave a maximum relative error of 0.044% (Figure 12), but with a value of $c = 2$ rather than one. As before, the addition of the polynomial term does not improve the evaluation of the normal derivative. The use of the TPS^3 function with or without the polynomial term does not produce accurate results, yielding a maximum relative error bigger than 40%.

Neumann conditions

Let us now consider a boundary value problem of the second kind (Neumann condition) defined over the unit circle, centered as before at the point $(1, 1)$. From the uniqueness of the solution of the present problem, it requires an additional condition; we chose this to be the value of the potential at the centre of the circle. Using the MQ function with the Gauss solver, the best result was obtained with the value of the shape parameter equal to two, yielding a maximum relative

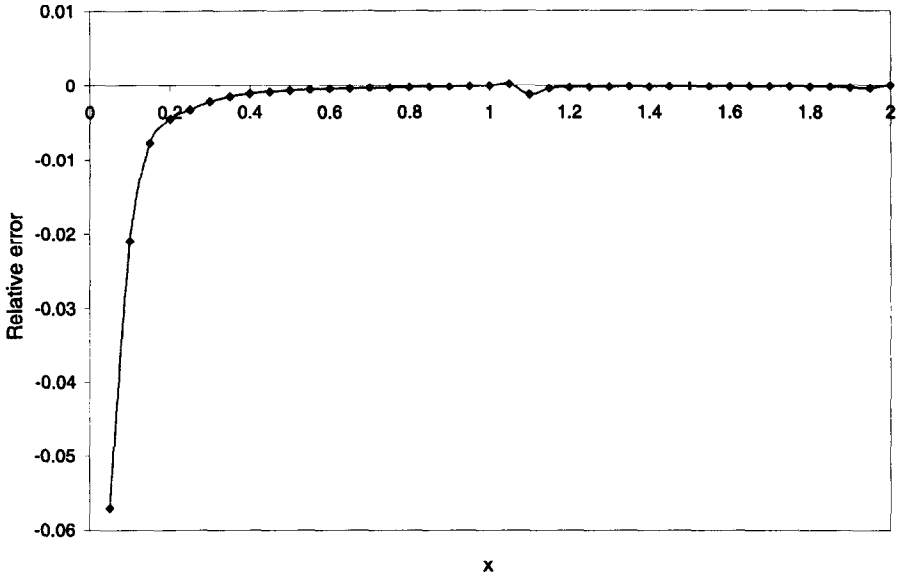

Figure 8. Relative error on the Dirichlet problem obtained with the unsymmetric method based on the TPS^3 function.

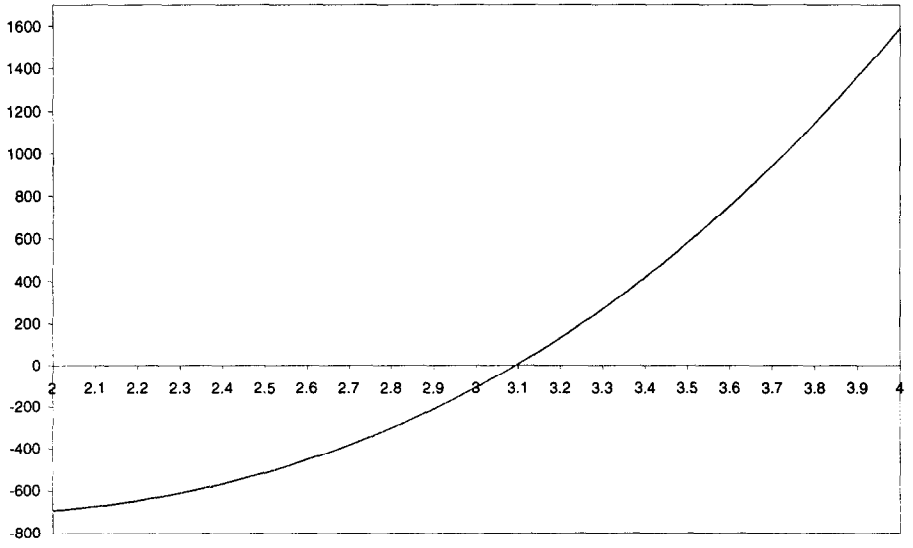

Figure 9. Analytical values of the potential on the line $y = 3$ for a circle centre at the point $(3, 3)$.

error of 0.025% (Figure 13). No significant improvement was observed by adding the polynomial term.

A similar result to the one obtained with the Gauss solver was found when the GMRES solver was employed, but the best value of the shape parameter was one instead of two. The use of the TPS^3 function with and without the polynomial term always produced very bad results independently of the solver used.

Mixed boundary conditions

Let us now consider the problem where in some part of the boundary, the value of the function is given and in the remaining part, the value of its normal derivative is known. The percentage of the perimeter in which the value of the function is assigned is indicated in Figure 14.

As before, we start our analysis with the MQ function with a shape parameter equal to one. In this case, the obtained relative error decreases as the percentage of the circumference where the

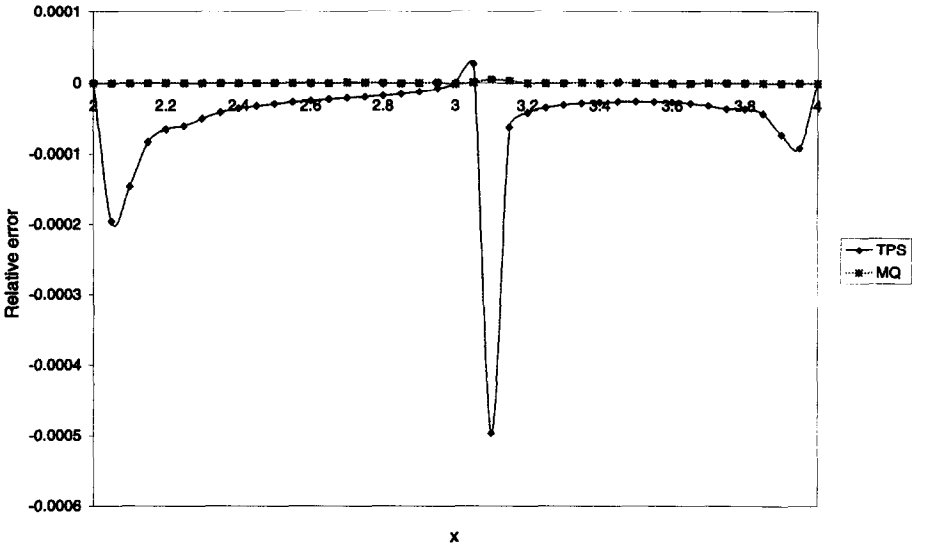

Figure 10. Comparison between the numerical results obtained with the MQ and the TPS^3 functions for a circle centered at the point $(3, 3)$.

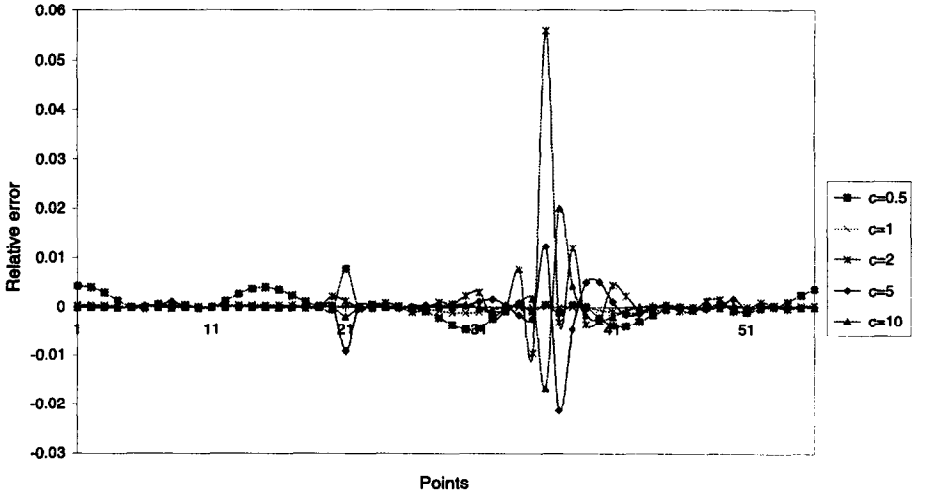

Figure 11. Relative error on the evaluation of the normal derivative obtained with the unsymmetric method based on the MQ function and solved with the Gauss solver.

function is defined increases. It is equal to 6.3% when the value of the function is given at the 5% of the circumference, but it is only 0.048% when the value of the function is assigned at 75% of the circumference (Figure 15). This behaviour was observed in each of the results obtained. No improvement was observed by increasing the value of the shape parameter to two. The use of the TPS^3 function with or without the polynomial term does not produce good results, even in the case when the value of the function was defined at 75% of the circumference. For such a case, the maximum relative error was 3.5%, instead of the 0.048% obtained with the MQ function.

2.1.2. Convection-diffusion equation

In this section, we consider the steady-state convection-diffusion equation in a rectangular domain $[1 \times 0.6]$. For simplicity, we chose the diffusion and convective coefficients as constants with the convective term only in the x_1 direction. The PDE to be solved has the form

$$D\frac{\partial^2 \Phi}{\partial x_j^2} - u\frac{\partial \Phi}{\partial x_1} = 0,$$

where D is the diffusion coefficient, u is the velocity in the x_1 direction, and Φ is the potential.

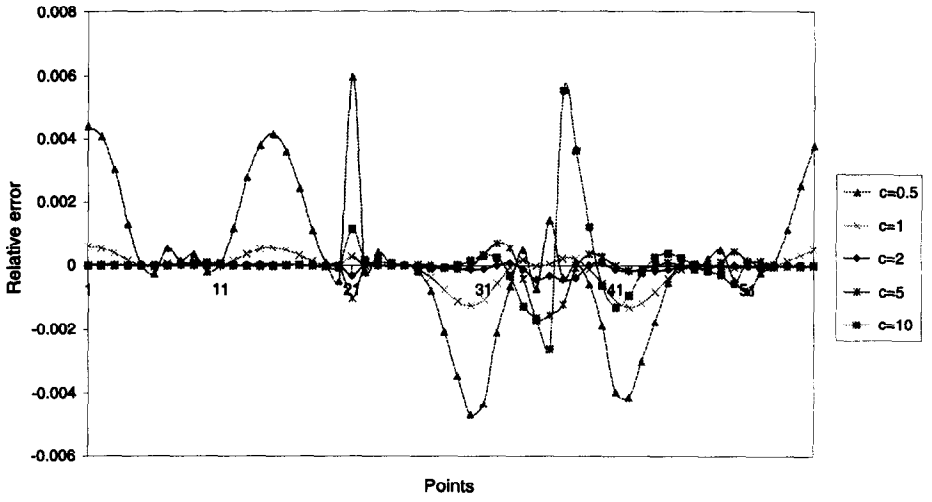

Figure 12. Relative error on the evaluation of the normal derivative obtained with the unsymmetric method based on the MQ function and solved with the GMRES iterative solver.

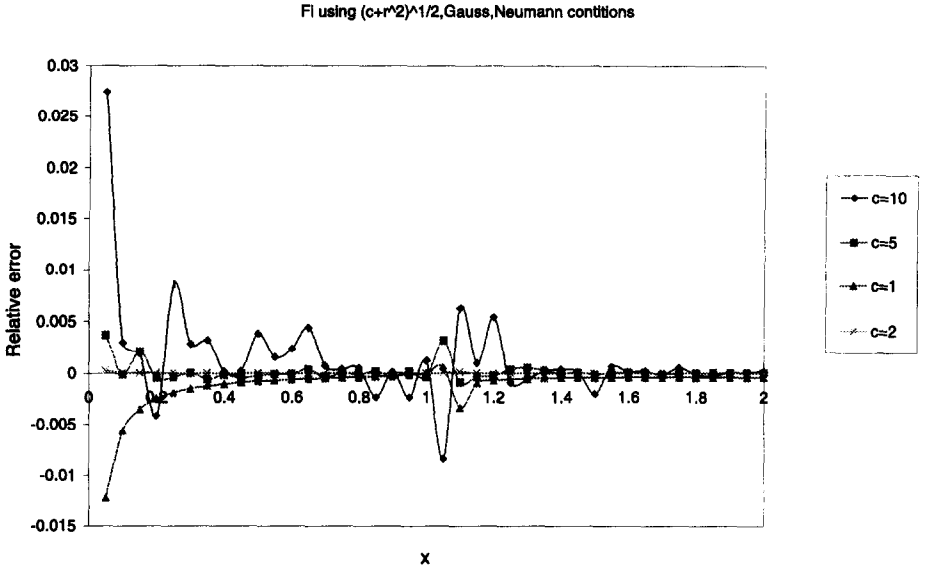

Figure 13. Relative error on the Neumann problem obtained with the unsymmetric method based on the MQ function and solved with the Gauss solver.

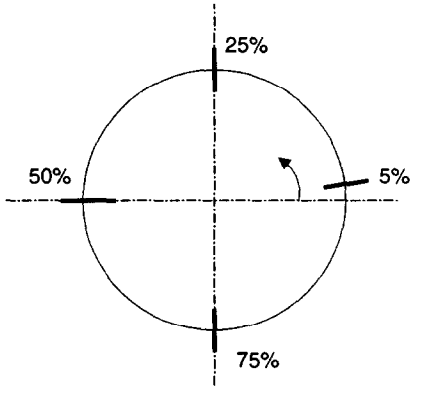

Figure 14. Definition sketch of the percentage of the perimeter of the circumference where the Dirichlet condition is prescribed.

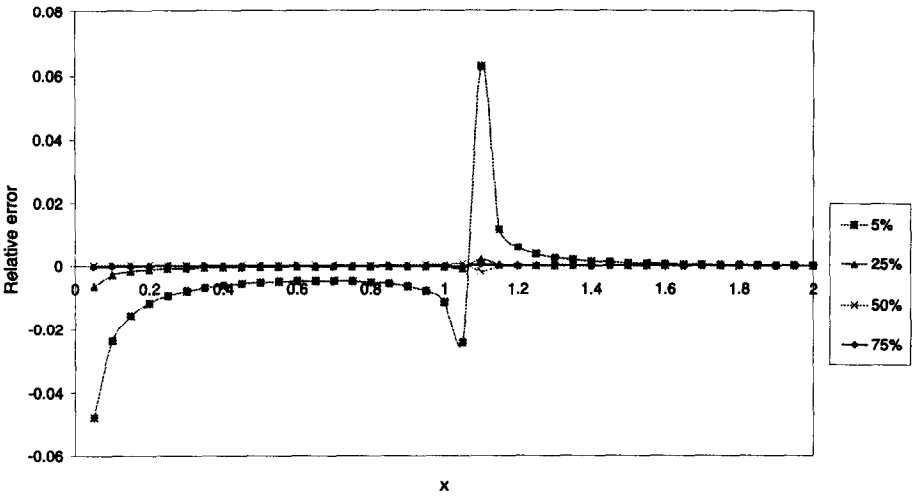

Figure 15. Relative error on the mixed boundary value problem obtained with the unsymmetric method based on the MQ function and solved with the Gauss solver.

The potential Φ has to satisfy the following boundary conditions:

$$\begin{aligned} \frac{\partial \phi}{\partial y} &= 0, \quad 0 \le x \le 1, \quad y = 0, \\ \frac{\partial \phi}{\partial y} &= 0 \quad 0 \le x \le 1, \quad y = 0.6, \\ \phi &= 1, \quad 0 \le y \le 0.6, \quad x = 0, \\ \phi &= 2, \quad 0 \le y \le 0.6, \quad x = 1. \end{aligned} \tag{16}$$

The analytical solution of the above problem is

$$\Phi(x) = 2 - \frac{1 - \exp[u(x-1)]}{1 - \exp(-u)}.$$

In a convection-diffusion problem, the parameter that describes the relative influence of the convective and the diffusive components is the Péclet number, $P_e = uL/D$, where u is the velocity, L a reference length, and D the diffusivity. In this section, we will solve the above problem for different value of the Péclet number (for simplicity D and L are assigned a unit value).

Our first mesh consists of 81 uniformly distributed collocation points, 36 on the boundary and 45 in the interior (Figure 16). Let us first analyze our results when the TPS^3 function plus the polynomial term were employed. We start with a value of the velocity $u = 1$. In this case, as can be seen from Figure 17, there is no appreciable difference between the analytical and the numerical solutions, and the relative error was smaller than $10^{-2}\%$. By increasing the value of the velocity to 10, we noticed that some small differences appeared (Figure 18) with a maximum relative error smaller than 5%. For $u = 100$, some oscillations are present and the numerical solution is far from the analytical one (Figure 19). This type of oscillation is also typical for other numerical schemes, such as the FMD and FEM, for such high value of the Péclet number.

When the MQ function, with the polynomial term and a shape parameter $c = 1$, was employed, excellent results were found for values of the velocity $u = 1$ and $u = 10$ (see Figures 20 and 21) with a relative error of the order of $10^{-2}\%$. However, we still obtained bad results (worse than when the TPS^3 was employed) when $u = 100$, but in this case without the oscillations (Figure 22). Similar results to those obtained with the TPS^3 function were found with the value of $c = 2$.

We tried to increase the accuracy of the solution by increasing the number of collation points, 277 uniformly distributed collocation points of which 68 where at the boundary and 209 inside the domain (Figure 23). When the TPS^3 function with the polynomial term was used, good

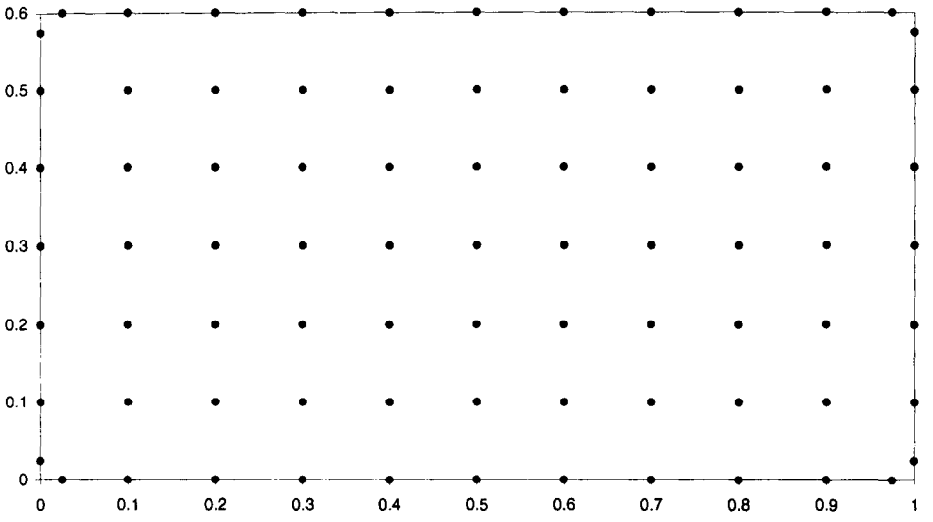

Figure 16. Distribution of 81 collocation points.

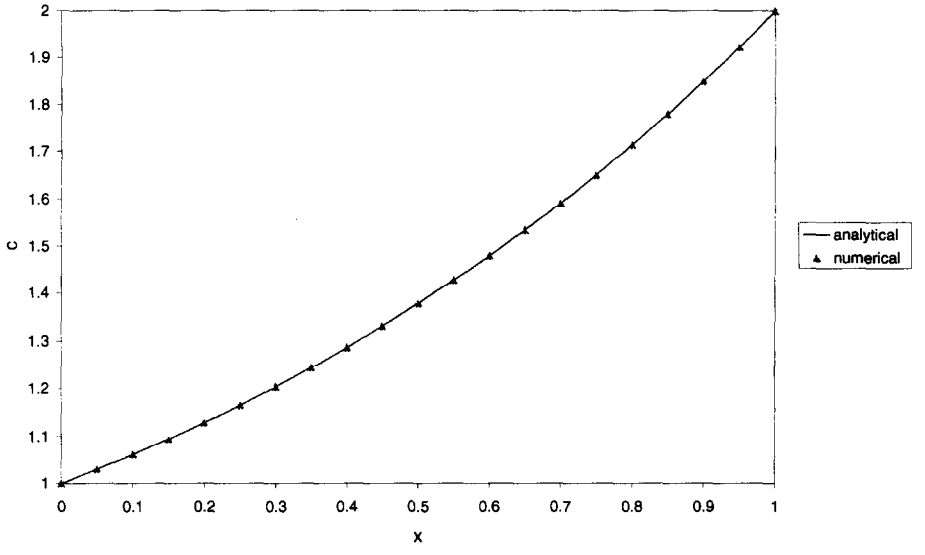

Figure 17. Comparison between the analytical and numerical solutions obtained with the unsymmetric method based on the TPS^3 function plus the polynomial term with the distribution of 81 collocation points. For the case of $u = 1$.

results were obtained for $u = 1$ and $u = 10$, but not for $u = 100$, Figure 24, where again the classical oscillations were present; however, this time the amplitude of the oscillations is smaller than those obtained when only 81 collocation points were employed and the numerical solution oscillates around the analytical one. By further increasing the number of collocation points to 533, 104 on the boundary and 429 inside the domain (Figure 25), it was possible to slightly improve the solution for $u = 100$. In this case, we were able to eliminate the oscillations, but a considerable error is still present (Figure 26). With this dense number of collocation points, we also used the MQ function with the polynomial and a shape parameter $c = 1$. For the case of $u = 100$, no improvement was observed with respect to the previous results obtained with MQ function with the less refined collocation points.

The difficulty encountered with the solution of this problem at high values of the Péclet number lies in the nature of the analytical solution, because for such a high value of this number the potential is constant and equal to one almost until $x = 1$, where it suddenly increases to the value of two. It is not easy to predict this type of behaviour numerically. Two other attempts

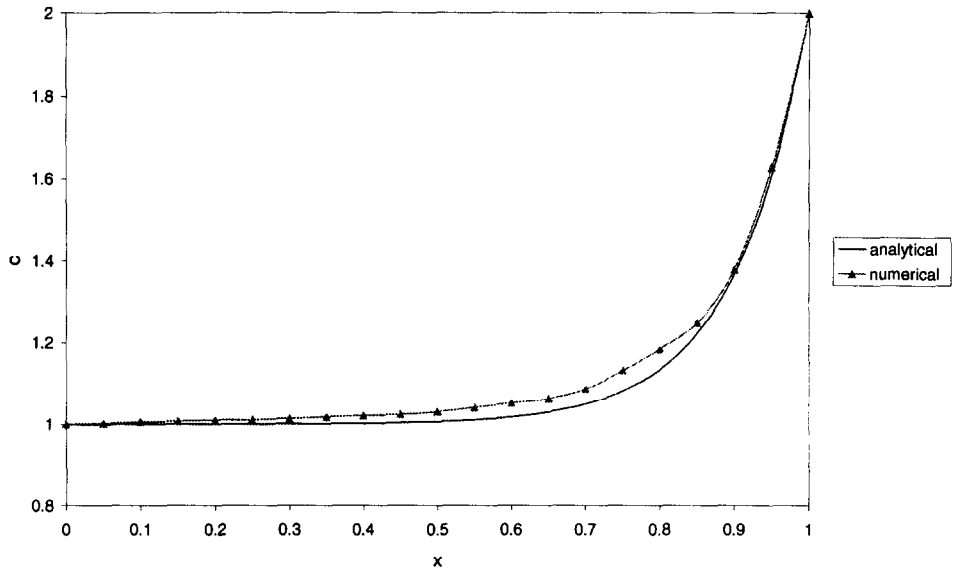

Figure 18. Comparison between the analytical and numerical solutions obtained with the unsymmetric method based on the TPS^3 function plus the polynomial term with the distribution of 81 collocation points. For the case of $u = 10$.

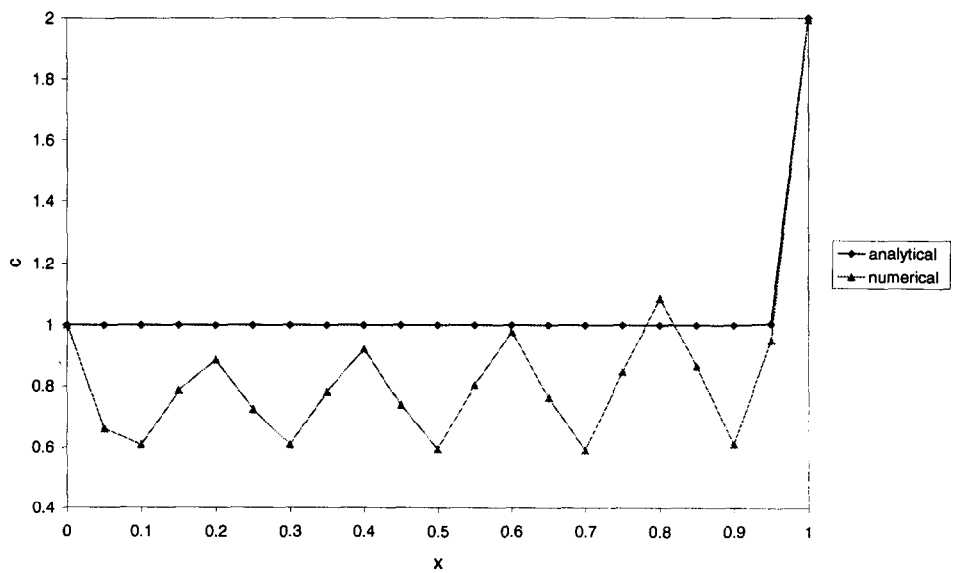

Figure 19. Comparison between the analytical and numerical solutions obtained with the unsymmetric method based on the TPS^3 function plus the polynomial term with the distribution of 81 collocation points. For the case of $u = 100$.

were made to solve this problem for $u = 100$ using both interpolation functions, with and without the polynomial term, with a nonuniform distribution of collocation points, with higher density of points in the region where the solution changes from the value of one to two, but we did not succeed.

2.2. Symmetric Method

In this section, we will repeat all the numerical examples tested with the unsymmetric method in order to see where and when there are differences between the two approaches. In addition, we will solve the problem of a semi-infinite continuous rectangular plane source in a uniform convective flow. We will again test the behaviour of the two different solvers and the use of

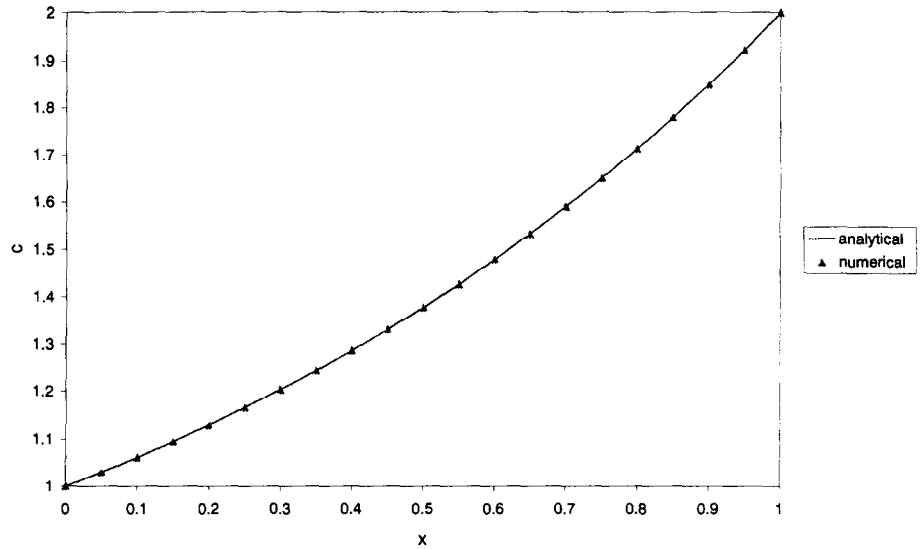

Figure 20. Comparison between the analytical and numerical solutions obtained with the unsymmetric method based on the MQ function with the distribution of 81 collocation points. For the case of $u = 1$.

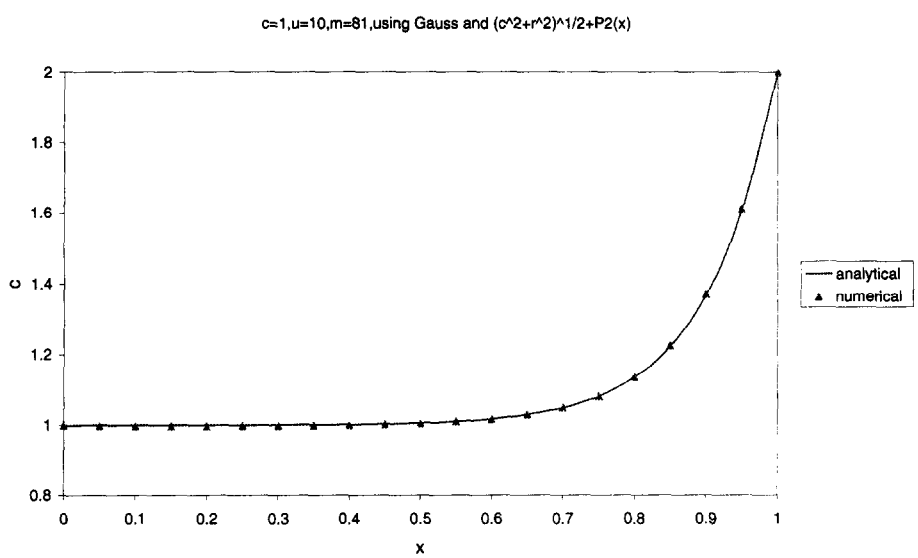

Figure 21. Comparison between the analytical and numerical solutions obtained with the unsymmetric method based on the MQ function with the distribution of 81 collocation points. For the case of $u = 10$.

both the thin plate splines and the multiquadric functions, but in this case, we always use the polynomial term according to the solvability condition of system (10).

2.2.1. Laplace's equation

In contrast to the unsymmetric method, where it was required to use at least a generalized thin plate spline function of the order $m = 3$, with a symmetric method it is necessary to use at least a generalized thin plate spline function of the order $m = 4$, TPS^4, in order to avoid the singularity at $r = 0$ appearing from the biharmonic operator in the matrix (10). Our previous results with the unsymmetric method did not have significant changes when the TPS^4 function was used instead of the TPS^3 function.

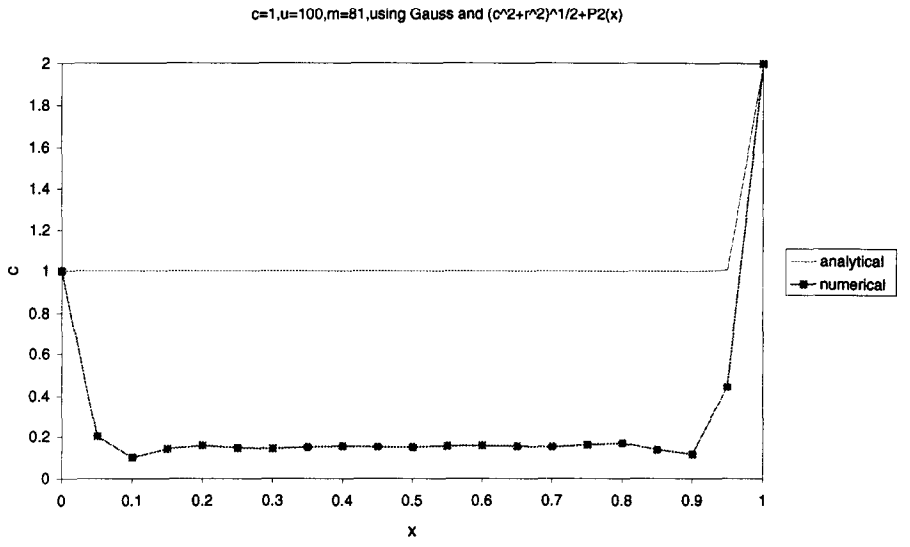

Figure 22. Comparison between the analytical and numerical solutions obtained with the unsymmetric method based on the MQ function with the distribution of 81 collocation points. For the case of $u = 100$.

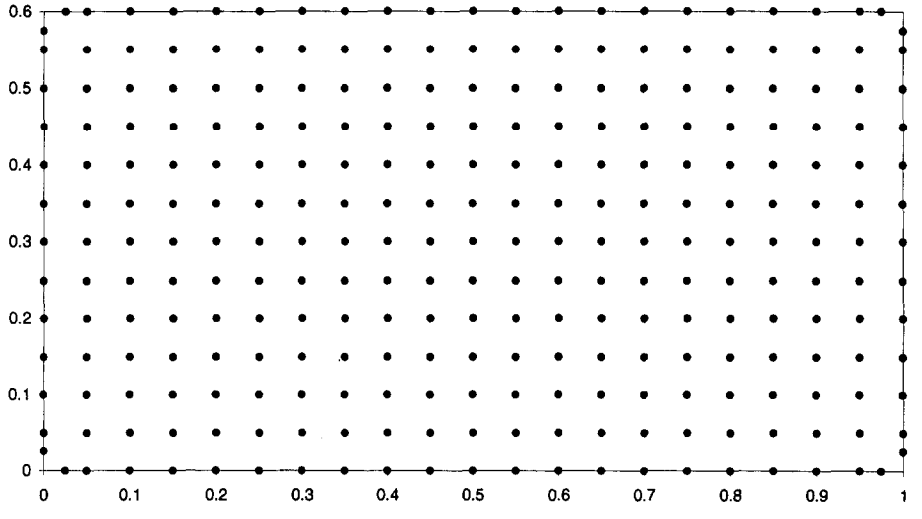

Figure 23. Distribution of 277 collocation points.

(I) Dirichlet boundary condition in a rectangular domain

This time we start directly with the example of 273 uniformly distributed collocation points. Using the MQ function with $c = 1$, a maximum relative error of 1.38% was found near the vertical walls and on the line $y = 0.3$ (Figure 27). When we used the TPS^4 function, a maximum relative error of 0.8% on the line $y = 0.5$ was found (Figure 28). This time the maximum error was observed at the middle part of the rectangle instead of on the two sides.

For this example, both the unsymmetric and the symmetric methods gave the same order of accuracy. Figure 29 shows a comparison between the analytical and the numerical solutions for each horizontal line of the domain including the boundaries.

(II) Circular domain

As before, we solved the Laplace equation in a circle domain for different types of boundary conditions. From our results, we can conclude that the symmetric approach seems to be more fruitful than the unsymmetric one, especially when using the TPS function. With the use of the

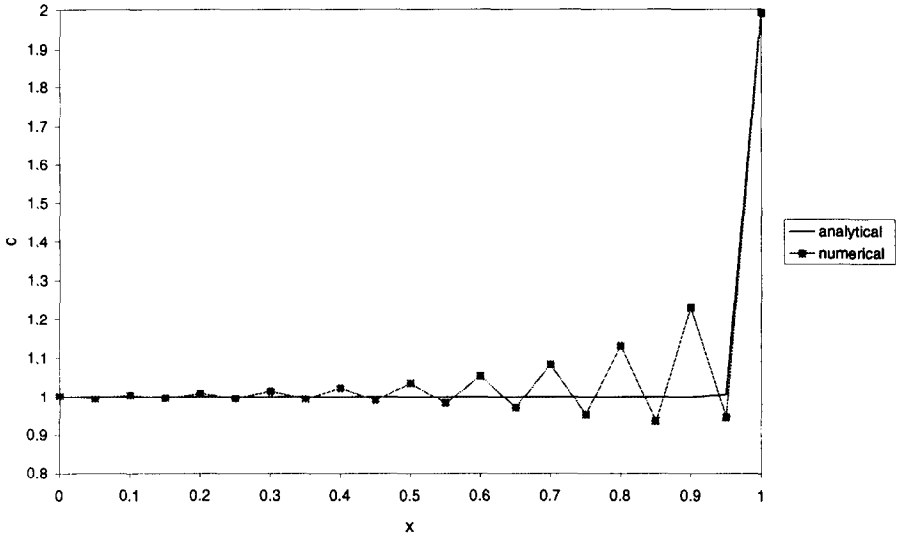

Figure 24. Comparison between the analytical and numerical solutions obtained with the unsymmetric method based on the TPS^3 function plus the polynomial term with the distribution of 277 collocation points. For the case of $u = 100$.

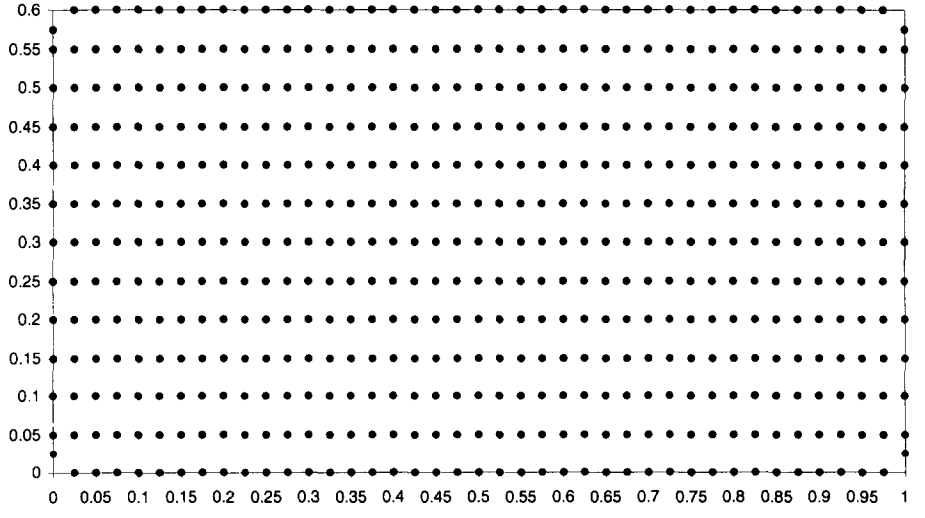

Figure 25. Distribution of 533 collocation points.

symmetric method, it was possible to find good results for all the different problems tested before in the circle of unit radius centered at the point $(1, 1)$, which was not always the case when the unsymmetric method was employed.

Dirichlet boundary condition

Using the MQ, a maximum relative error of $7 \cdot 10^{-4}\%$ was found for a value of the shape parameter $c = 5$ (Figure 30). Both solvers, i.e., the GMRES and Gauss, gave the same accuracy.

For this problem, both the MQ and the TPS^4 functions gave similar accuracy. When we used the TPS^4, a maximum relative error of $7 \cdot 10^{-5}\%$ was obtained. A small difference was observed when different solvers were employed (see Figure 31), but the improvement was insignificant when compared to the high precision of the results. In this case, the behaviour of the TPS^4 with the symmetric method was better than with the unsymmetric method, with which the relative error was found to lie between 5.7%, near the vertical axis, to 0.45%, close to the point $(1, 1)$ (Figure 8).

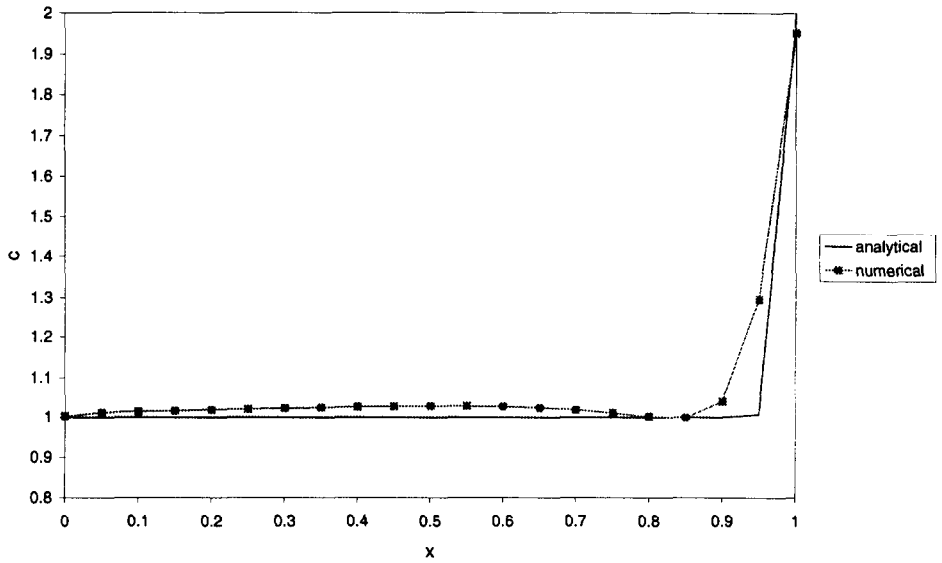

Figure 26. Comparison between the analytical and numerical solutions obtained with the unsymmetric method based on the TPS^3 function plus the polynomial term with the distribution of 533 collocation points. For the case of $u = 100$.

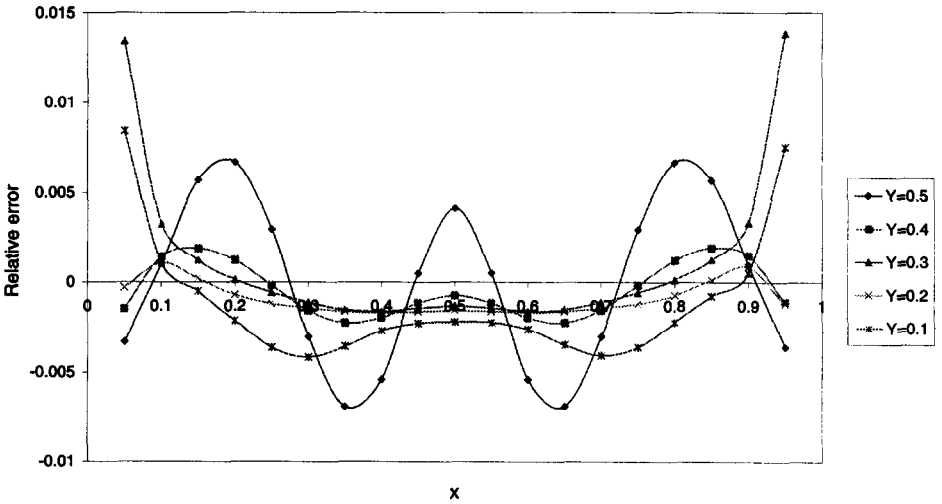

Figure 27. Relative error obtained with the symmetric method based on the MQ function with the distribution of 273 collocation points.

Normal derivative of a Dirichlet problem

For the evaluation of the normal derivative of a Dirichlet boundary problem, the GMRES and Gauss solvers produced the same results for both MQ and TPS^4 functions. For the MQ, the best value of the shape parameter was $c = 5$, yielding to a maximum relative error of 0.023% (Figure 32). The TPS^4 behaved worse than the MQ, yielding to a maximum relative error of 3.2% (Figure 33). However, the use of the multiquadric and the thin plate spline functions with the symmetric approach gave more accurate results than those obtained with the unsymmetric method.

Neumann conditions

Like before, as well as defining the Neumann boundary conditions over the unit circle, we also gave the value of the potential at the centre of the circle in order to guarantee the uniqueness of the solution of the problem. This time, the GMRES and the Gauss solvers gave different

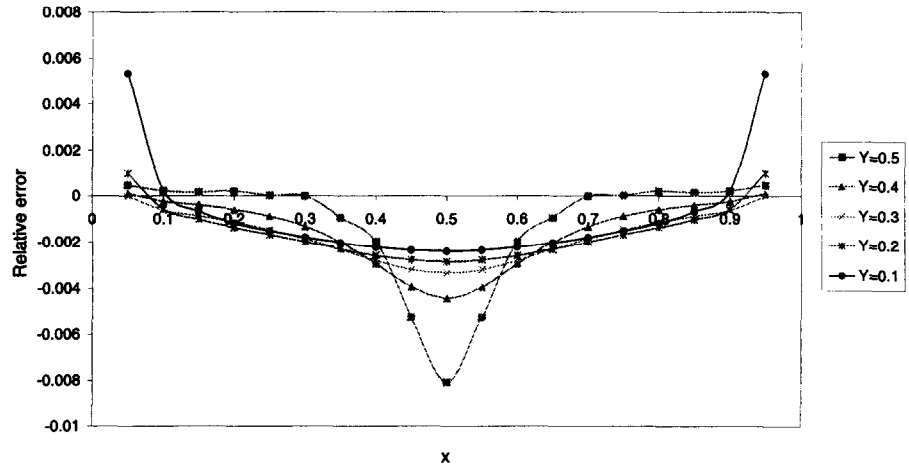

Figure 28. Relative error obtained with the symmetric method based on the TPS function with the distribution of 273 collocation points.

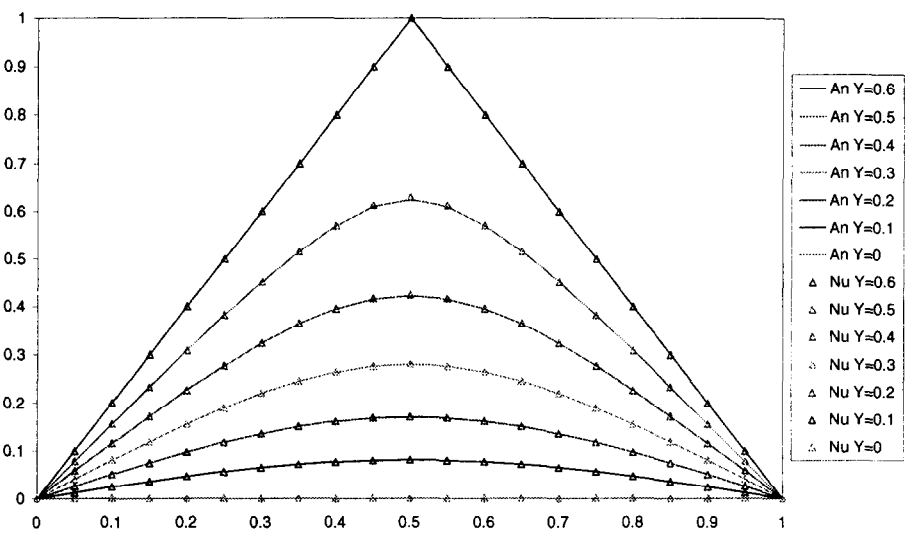

Figure 29. Comparison between the analytical and numerical solutions obtained with the symmetric method.

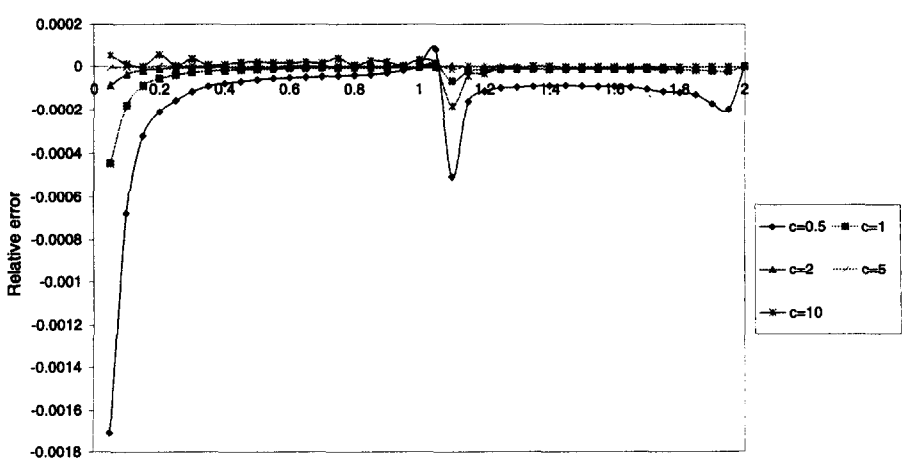

Figure 30. Relative error on the Dirichlet problem obtained with the symmetric method based on the MQ function.

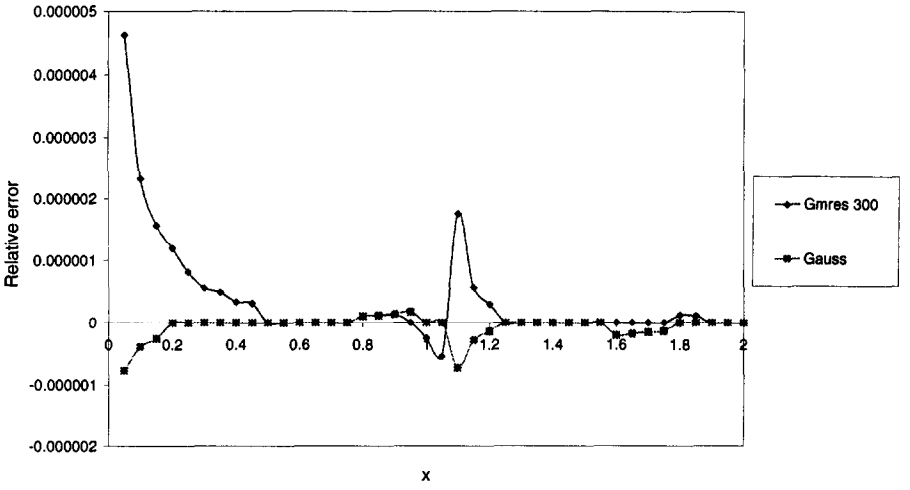

Figure 31. Relative error on the Dirichlet problem obtained with the symmetric method based on the TPS function.

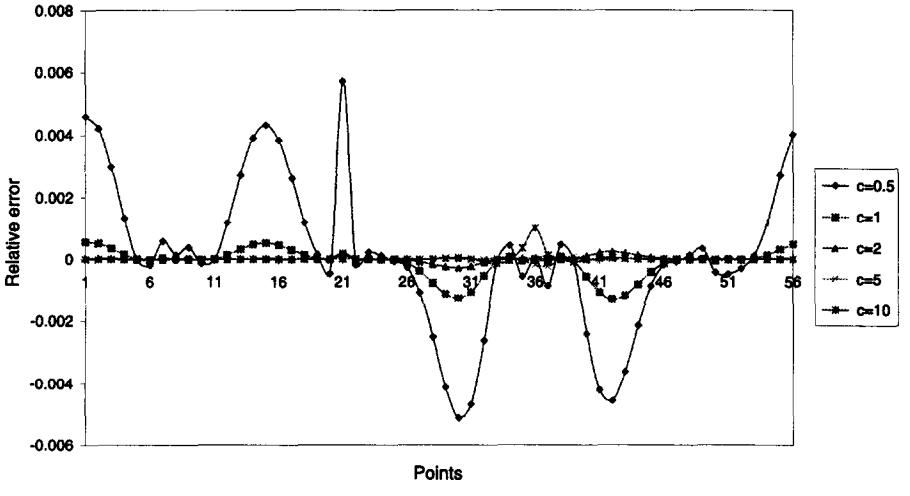

Figure 32. Relative error on the evaluation of the normal derivative obtained with the symmetric method based on the MQ function.

results, the latter being the more accurate. However, with both solvers, the best result was found with the same value of the shape parameter, $c = 2$. Using the MQ and the GMRES solver, a maximum relative error of 0.7% was obtained (Figure 34). When the Gauss solver was employed, a maximum relative error of 0.006% was found (Figure 35).

Different behaviour of the two solvers was again noticed when the TPS^4 was employed. The obtained maximum relative error with the GMRES solver was 0.011% and with the Gauss solver was 0.0043% (Figure 36). As in the previous example, the symmetric method gave more accurate results than the unsymmetric one, in particular, when the thin plate spline function was employed, for which the unsymmetric method did not work.

Mixed boundary conditions

The last test with the circle domain was carried out for a problem with mixed boundary condition. As with the unsymmetric method, for this case, the GMRES and the Gauss solvers gave almost the same accuracy. Using the MQ with $c = 1$, we obtained a maximum relative error of 0.16% when the value of the function was defined over 5% of the circumference (Dirichlet condition). It, however, decreased to 0.06% when the value of the function was assigned over 75% of the circumference (Figure 37). Other values of the shape parameter were tested, but no

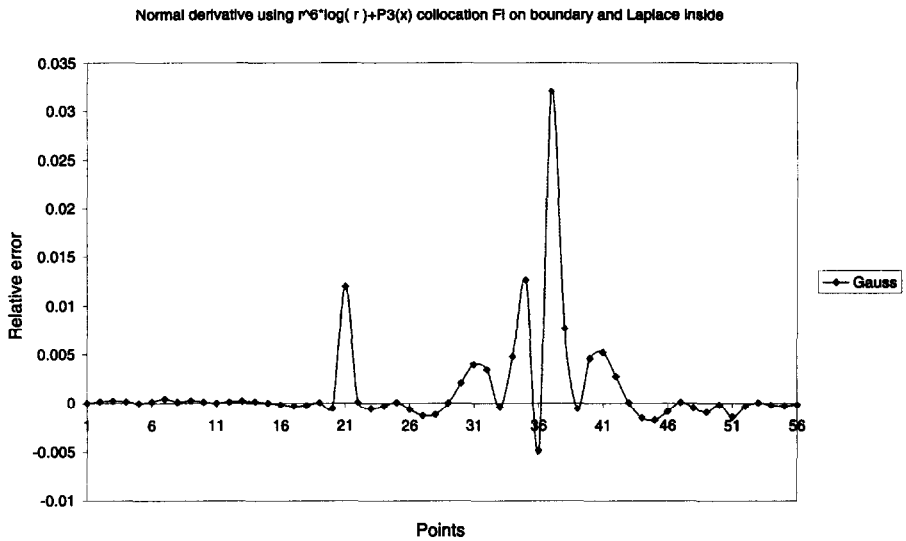

Figure 33. Relative error on the evaluation of the normal derivative obtained with the symmetric method based on the TPS function.

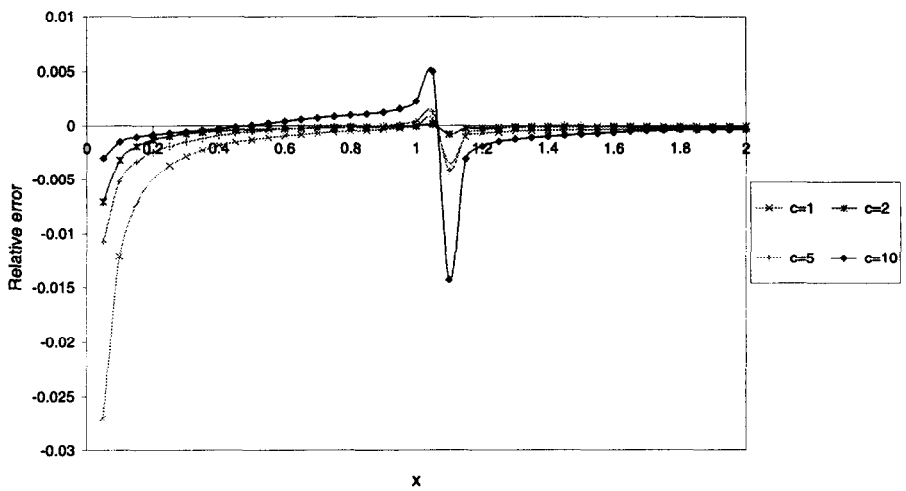

Figure 34. Relative error on the Neumann problem obtained with the symmetric method based on the MQ function and solved with the GMRES iterative solver.

significant improvements were observed. When the TPS^4 was used, we found a maximum relative error of 1.26% when the value of the function was assigned over 5% of the circumference and a value of 0.08% when the function was prescribed over 75% of the circumference (Figure 38).

2.2.2. Convection-diffusion equation

This is the last example solved with the symmetric method that we compare to the unsymmetric method; it again deals with the influence of the Péclet number, $P_e = vL/D$, on the numerical solution of convection-diffusion problems.

First, we tested a mesh of only 81 collocation points (as we did with the unsymmetric method (Figure 16)), which gave good results for $u = 1$ and $u = 10$, but not for $u = 100$. Then, we used a mesh of 277 uniformly distributed collocation points (Figure 23) in order to predict the solution for the case of $u = 100$. For all the cases tested, both solvers employed (GMRES and GAUSS) gave almost the same accuracy.

Using the MQ with a shape parameter $c = 1$ in the case of a convective velocity equal to 100, we found that the numerical solution follows the analytical one, but with a value of almost 1.1 instead of one (a relative error of 10%) in the region of constant potential, i.e., from $x = 0$ to

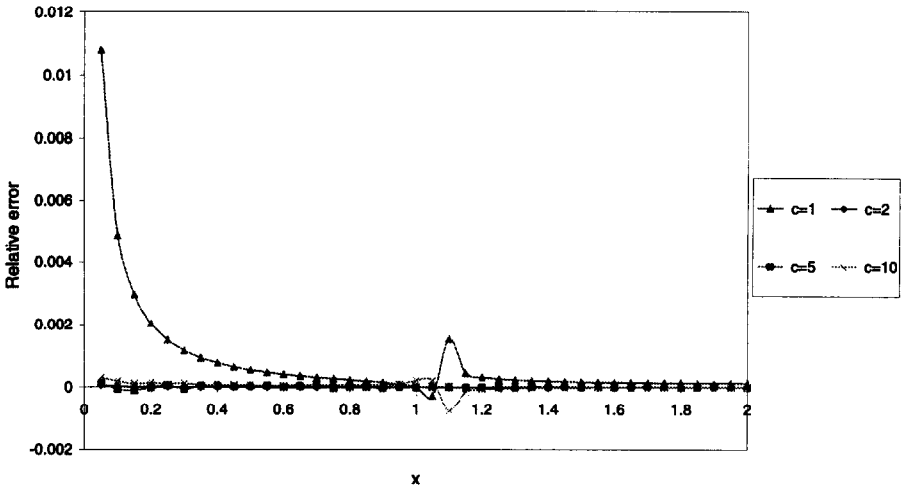

Figure 35. Relative error on the Neumann problem obtained with the symmetric method based on the MQ function and solved with the Gauss solver.

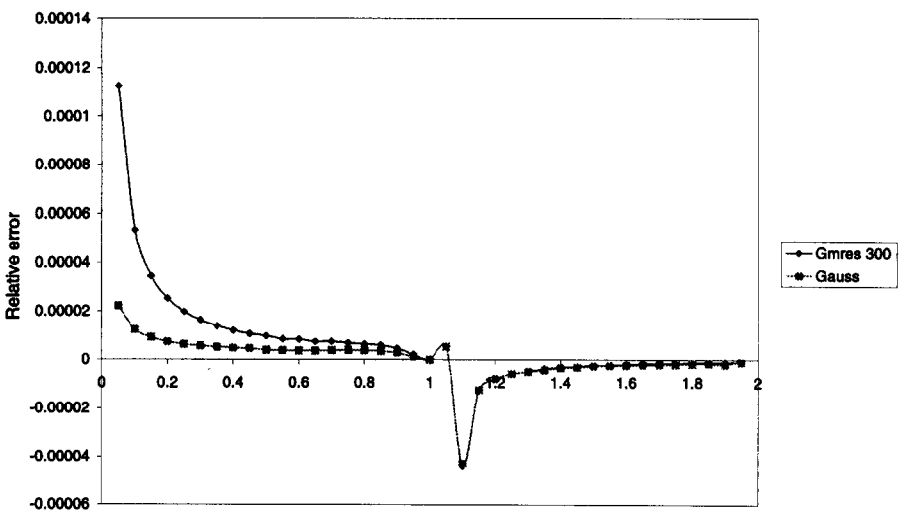

Figure 36. Relative error on the Neumann problem obtained with the symmetric method based on the TPS function.

almost $x = 0.95$ (see Figure 39). A similar result was obtained when the TPS^4 function was employed, but the error on the region of constant potential was larger, a relative error of 35% (see Figure 40). It is important to underline that we did not obtain any numerical oscillations, which usually appear when other numerical schemes, such as the FDM or FEM, and also were presented in our previous solution with the unsymmetric method. For this reason, as well as to avoid the problem of finding an optimal value for the shape parameter, in our following tests we only used the TPS^4 function.

By increasing the number of collocations points to 533, we obtain a numerical solution that almost coincides with the analytical one (see Figure 41), resulting in a maximum relative error of 0.55% in the region between $x = 0.95$ and $x = 1$, where the solution suddenly changed from the value of one to two, and less than 0.01% in the region of constant potential. With the use of 624 nonuniformly distributed collocation points (Figure 42), we were able to practically eliminate this small difference (see Figure 43), resulting in a relative error smaller than 0.01% everywhere. We also tested several nonuniform distributions of collocation points, but none of the results were better than the one obtained with the 624 nonuniform distribution.

As can be observed, for this type of problem, the results obtained with the symmetric method outperform those obtained with the unsymmetric, in particular, when the thin plate spline func-

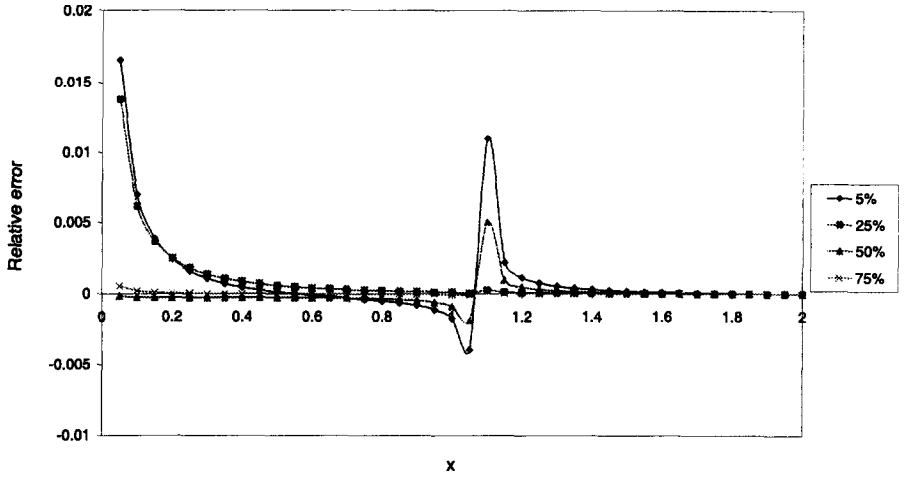

Figure 37. Relative error on the mixed boundary value problem obtained with the symmetric method based on the MQ function and solved with the Gauss solver.

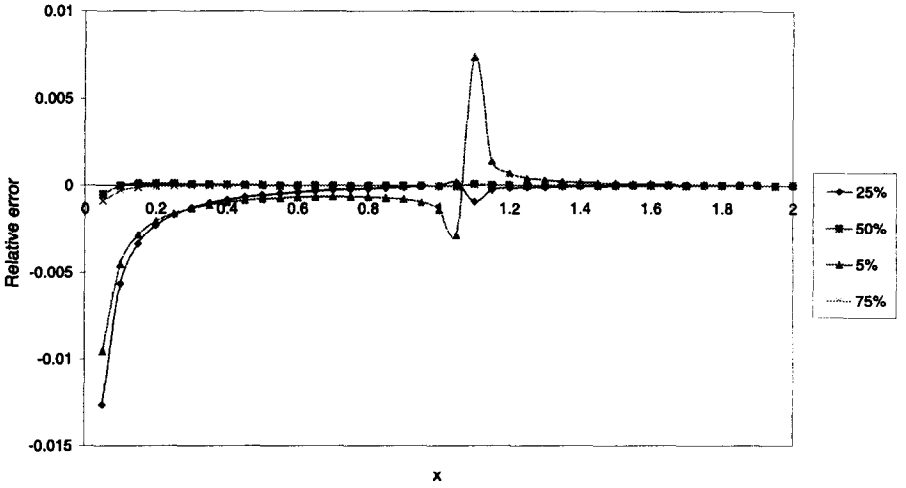

Figure 38. Relative error on the mixed boundary value problem obtained with the symmetric method based on the TPS function and solved with the Gauss solver.

tion is employed. This time we were able to obtain excellent results even in the case of very high Péclet number, which is a difficult task for any numerical scheme.

Rectangular plane source in a uniform convective flow

From the previous numerical examples comparing the symmetric and the unsymmetric methods, we can conclude that the first in general performs better, especially when using the thin plate spline interpolating functions. For both methods, symmetric and unsymmetric, the use of the MQ function with a proper selection of the shape parameter almost always produced slightly better results than the ones obtained with the TPS, but it requires the additional work of finding the optimum value of this parameter.

Given the excellent results obtained with the symmetric method based upon the thin plate spline interpolation functions for solving convection-diffusion problems, as a final example we will consider the problem of a two-dimensional plane source of width equal to b perpendicular to the fluid motion. Uniform flow velocity in the x_1 direction and constant decay term are assumed. Under this condition, the governing equation that we need to solve has the following form:

$$u\frac{\partial \Phi}{\partial x_1} = D\frac{\partial^2 \Phi}{\partial x_j^2} - k\Phi. \tag{17}$$

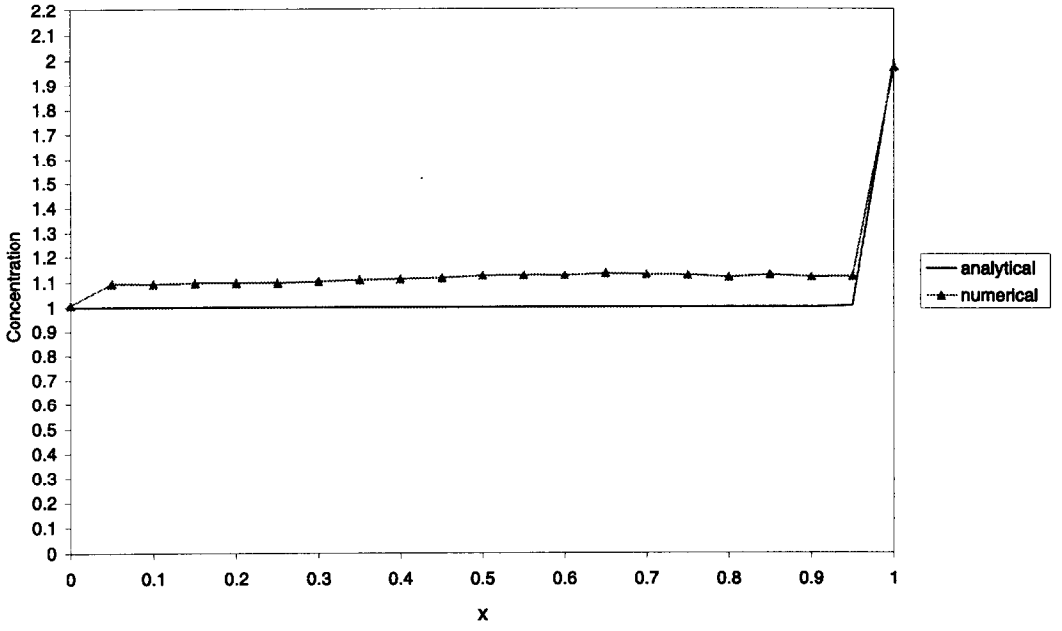

Figure 39. Comparison between the analytical and numerical solutions obtained with the symmetric method based on the MQ function with the distribution of 277 collocation points. For the case of $u = 100$.

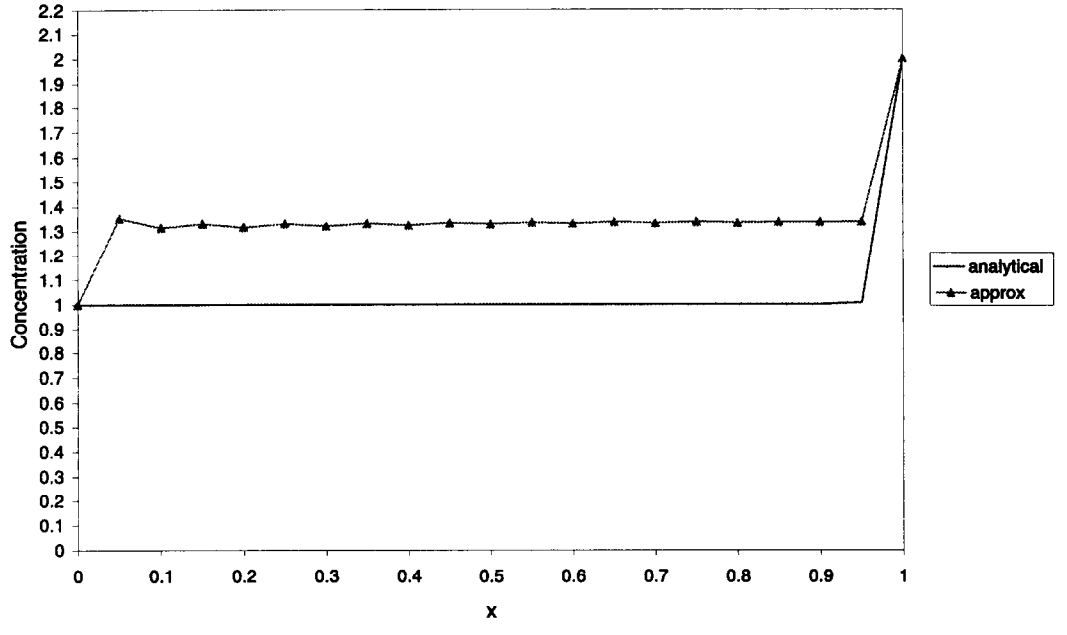

Figure 40. Comparison between the analytical and numerical solutions obtained with the symmetric method based on the TPS function with the distribution of 277 collocation points. For the case of $u = 100$.

The boundary conditions of the problem are

$$\Phi = \Phi_0, \qquad \frac{-b}{2} \leq y \leq \frac{b}{2}; \qquad x = 0,$$

$$\Phi = 0, \qquad -\infty \leq y \leq \frac{-b}{2}; \qquad \frac{b}{2} \leq y \leq \infty : x = 0,$$

$$\Phi \to 0, \qquad \text{as } R = \sqrt{x^2 + y^2} \to \infty, \quad x \geq 0.$$

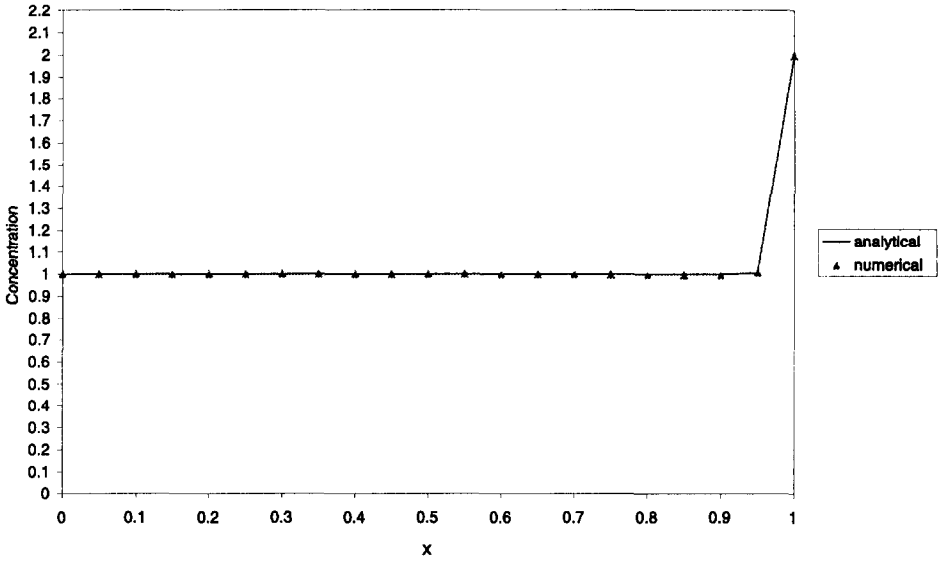

Figure 41. Comparison between the analytical and numerical solutions obtained with the symmetric method based on the TPS function with the distribution of 533 collocation points. For the case of $u = 100$.

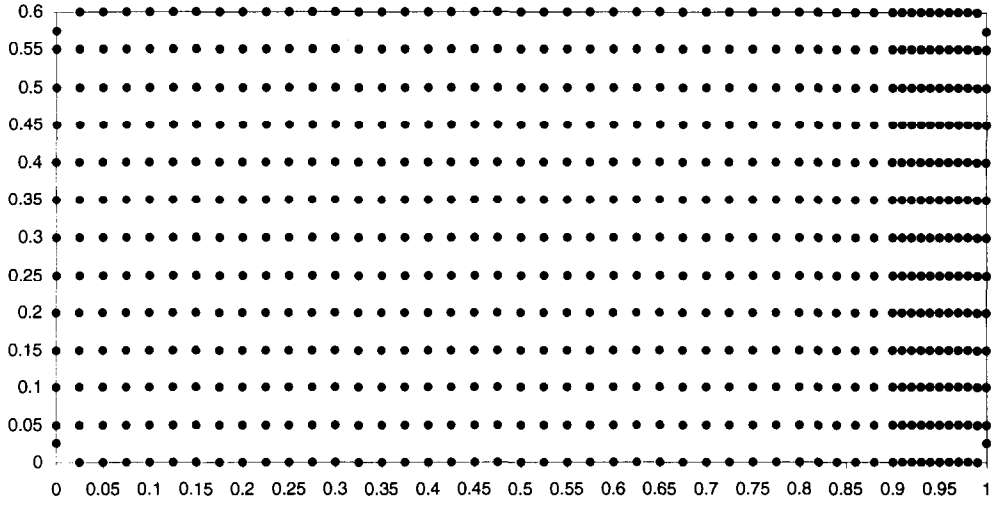

Figure 42. Nonuniform distribution of 624 collocation points.

The analytical solution of this problem is

$$\frac{\Phi(\mathbf{x})}{\Phi_0} = \frac{1}{2} e^{(-kx/u)} \left[\operatorname{erf}\left(\frac{y + b/2}{2} \sqrt{\frac{u}{Dx}} \right) - \operatorname{erf}\left(\frac{y - b/2}{2} \sqrt{\frac{u}{Dx}} \right) \right],$$

where erf is the error function.

At a distance d measured from the source, the maximum value of the potential lays at the horizontal axis $y = 0$, and is given by

$$\frac{\Phi_{\max}}{\Phi_0} = e^{(-kd/u)} \operatorname{erf}\left(\frac{b}{4} \sqrt{\frac{u}{Dd}} \right).$$

Two different strategies were implemented. In the first instance, we simulated part of the complete half space, as shown in Figure 44, with artificial boundary conditions at the contours Γ_1, Γ_2, and Γ_3, as is usually done in the numerical solution of this type of problems. At the contours Γ_1 and Γ_3, we imposed the zero flux condition to guarantee symmetry, and at the

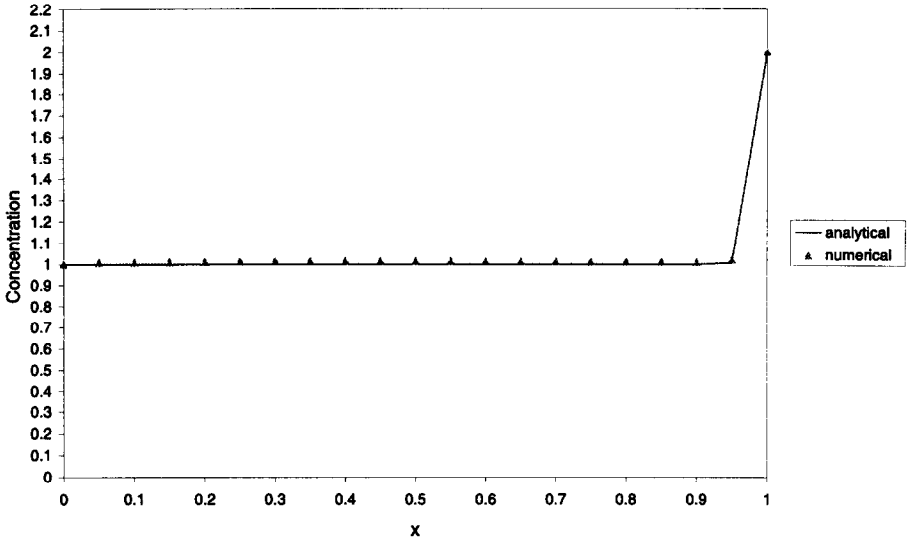

Figure 43. Comparison between the analytical and numerical solutions obtained with the symmetric method based on the TPS function with the distribution of 624 collocation points. For the case of $u = 100$.

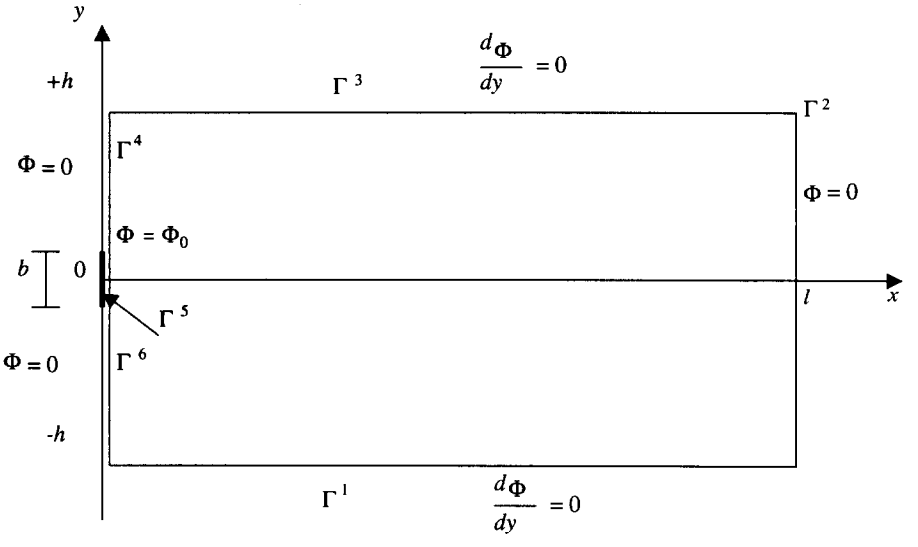

Figure 44. Definition sketch of the boundary conditions and problem domain for the nonfree boundary condition case.

boundary Γ_2, which is chosen far from the plane source, we imposed a value of zero to the potential, i.e., $\Phi = 0$.

In the second strategy, we did not assign any boundary conditions on Γ_2 (free boundary condition). In this case, the linear system to be solved is similar to the previous one, except for the condition on Γ_2, where we need to satisfy the original partial differential equation in the same way that it is done at the internal nodes.

First, we compared the analytical solution at the centre line of the plume, i.e., $\Phi_{\max}$, with the numerical results obtained with each of the two strategies. In our example, we choose the following values for the parameters: $l = 6$, $h = 5$, $b = \Phi_0 = D = 1$, $k = u = 10$.

We started our analysis using 267 uniformly distributed collocation points equally spaced in the x and y direction, $\Delta x = \Delta y = 0.5$. As can be seen from Figure 45, a better solution is obtained when the free boundary condition is applied at Γ_2 (shown in the figure as numerical FB). It is important to observe a type of mass reflection coming from the contour Γ_2, which is present in the

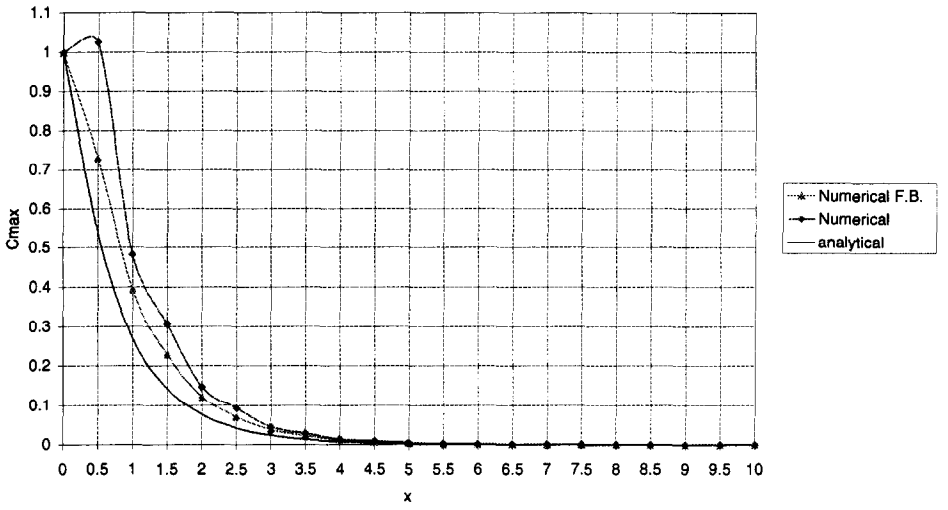

Figure 45. Comparison between the analytical maximum concentration and the numerical results obtained with the symmetric method with the uniform distribution of collocation point equally spaced at 0.5, free boundary condition (numerical FB), artificial boundary condition (numerical).

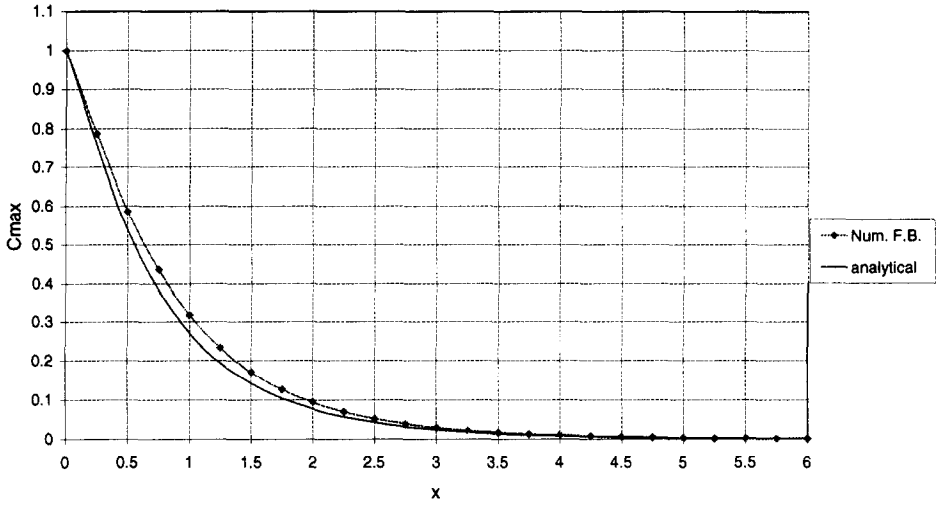

Figure 46. Comparison between the analytical maximum concentration and the numerical results with free boundary condition obtained with the symmetric method for a uniform distribution of collocation points equally spaced at 0.25.

solution when the artificial condition $\Phi = 0$ is imposed (shown in the figure as numerical). This irregularity does not appear with the other type of condition at Γ_2 (free boundary condition). The solution with the artificial boundary condition can be improved by allowing the contours Γ_2 to be further away from the origin, but at the expense of more computational cost. Since the strategy with the free boundary condition seems to work better than the other one, in the next tests, we will only consider this type of condition.

As a second test, we increased the number of collocation points by using a more dense uniform distribution of points with a spacing of 0.25 in both directions. As can be seen from Figures 46 and 47, this time the numerical solution is closer to the analytical one. In our last test, we further increased the density of collocation points by decreasing the spacing to 0.15 in both directions. As can be observed from Figure 48, a significant improvement was obtained with this distribution of points.

It is important to point out that the idea of imposing a free boundary condition instead of the classical artificial zero potential can also be used with the unsymmetric method.

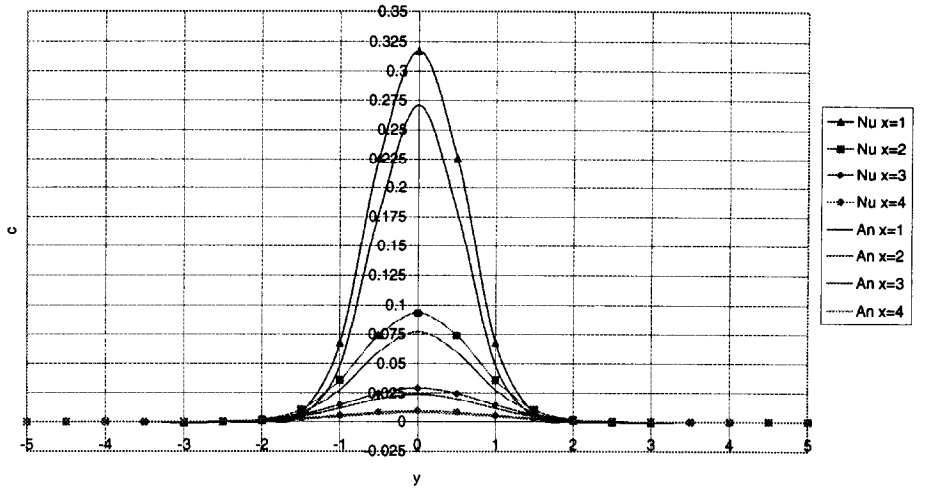

Figure 47. Comparison between the analytical cross section concentration profile and the numerical results obtained with the symmetric method with the uniform distribution of collocation points equally spaced at 0.25.

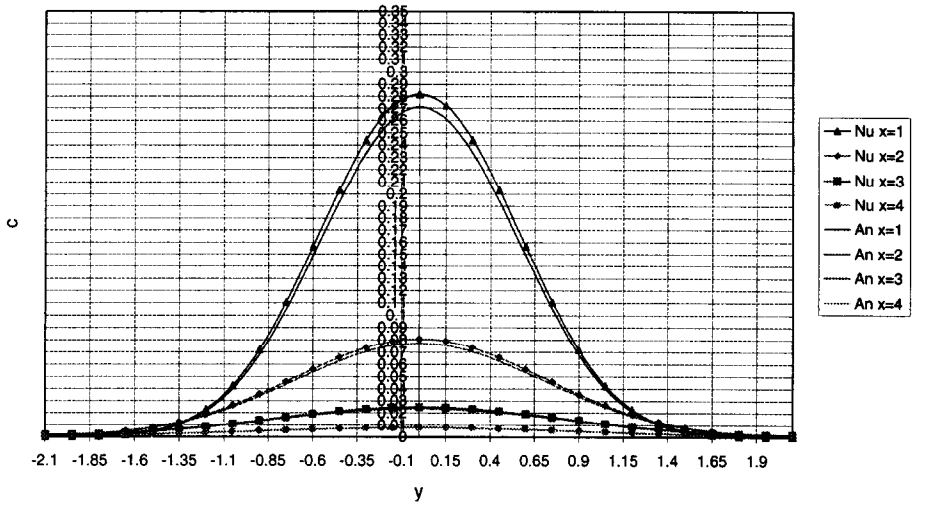

Figure 48. Comparison between the analytical cross section concentration profile and the numerical results obtained with the symmetric method with the uniform distribution of collocation points equally spaced at 0.15.

3. CONCLUSIONS

This work tests the efficiency of two new free mesh numerical schemes based on radial basis interpolation functions to solve partial differential equations. The first method tested was an unsymmetric method, and the second one, which appears to be more efficient, was a symmetric one. In order to understand the differences between these two approaches, we started our analysis by applying them to solve different boundary value problems for the two-dimensional Laplace equation. This allowed us to find out which radial basis function is more appropriate to use with each of the methods. To solve the linear system of equations that arises from the application of the two methods, we used the Gauss elimination method with partial pivoting and the GMRES iterative method. A series of test examples was carried out using the two approaches to solve a boundary value problem for the two-dimensional steady-state convection-diffusion equation with constant coefficients; particular attention was paid to problems with high Péclet number.

Both the symmetric and unsymmetric methods are relatively easy to implement when compared to classical methods, such as the FDE, FEM, and BEM. These two free mesh methods are

also straightforward to apply to three-dimensional problems; it is only necessary to use a 3-D distribution of points and the corresponding 3-D radial basis functions.

With the unsymmetric method, the MQ and the TPS functions were used with and without the polynomial term. No major improvements on the accuracy of the results were observed when the polynomial term was employed. The polynomial terms were always used when those functions, i.e., MQ and TPS, were employed in the symmetric method, in order to guarantee the solvability condition of the corresponding Hermitian matrix.

The use of the GMRES and the Gauss solver yields almost the same results when the TPS is used with both the symmetric and unsymmetric methods. However, this was not the case when the MQ function was employed. With the unsymmetric method, sometimes different results are obtained using different solvers, and in some cases no convergence was achieved. This does not happen with the symmetric method.

In general, we can say that the symmetric method outperforms the unsymmetric one. Using the symmetric method, it was always possible to obtain with the TPS function similar results to those obtained with the MQ function. Two main features about the results obtained in this work are worthy of special attention. First, with the symmetric method it was possible to solve convection-diffusion problems at a very high Péclet number without the need of any artificial damping term, and second, with these two approaches, symmetric and unsymmetric, it is possible to impose free boundary conditions for problems in unbounded domains.

REFERENCES

1. M.A. Golberg and C.S. Chen, *Discrete Projection Methods for Integral Equations*, Computation Mechanics Publications, Southampton, UK, (1997).
2. C.A. Micchelli, Interpolation of scattered data: Distance matrices and conditionally positive definite functions, *Constr. Approx.* **2**, 11–22, (1986).
3. R. Schaback, Multivariate interpolation and approximation by translates of a basis function, In *Approximation Theory VIII*, (Edited by C.K. Chui and L.L. Schumaker), pp. 1–8, (1995).
4. R. Franke, Scattered data interpolation: Tests of some methods, *Math. Comp.* **38**, 181–200, (1982).
5. S. Stead, Estimation of gradients from scattered data, *Rocky Mount. J. Math.* **14**, 265–279, (1984).
6. J. Duchon, Spline minimizing rotation—Invariant seminorms in Sobolev spaces, In *Constructive Theory of Functions of Several Variables, Lecture Notes in Mathematics, Volume 571, (Edited by W. Schempp and K. Zeller)*, pp. 85–100, Springer-Verlag, Berlin, (1977).
7. M.J.D. Powell, The uniform convergence of thin plate spline interpolation in two dimensions, *Numerische Mathematik* **68** (1), 107–128, (1994).
8. W.R. Madych and S.A. Nelson, Multivariable interpolation and conditionally positive definite functions—II, *Math. Comput.* **54**, 211–230, (1990).
9. A.E. Tarwater, A parameter study of Hardy's multiquadric method for scattered data interpolation, Technical Report UCRL-563670, Lawrence Livermore National Laboratory, (1985).
10. R. Franke, A critical comparison of some methods for interpolation of scattered data, Technical Report NPS-53-79-003, Naval Postgraduate School, (1975).
11. R.E. Carlson and T.A. Foley, The parameter R^2 in multiquadric interpolation, *Computers Math. Applic.* **21** (9), 29–42, (1991).
12. E.J. Kansa, Multiquadrics—A scattered data approximation scheme with applications to computation fluid-dynamics—I. Surface approximations and partial derivatives estimates, *Computers Math. Applic.* **19** (8/9), 127–145, (1990).
13. E.J. Kansa, Multiquadrics—A scattered data approximation scheme with applications to computation fluid-dynamics—II. Solution to parabolic, hyperbolic and elliptic partial differential equations, *Computers Math. Applic.* **19** (8/9), 147–161, (1990).
14. G.E. Fasshauer, Solving partial differential equations by collocation with radial basis functions, In *Proceedings of Chamonix*, (Edited by A. Le Méchauté *et al.*), pp. 1–8, Vanderbilt University Press, Nashville, TN, (1996).
15. Z. Wu, Hermite-Birkhoff interpolation of scattered data by radial basis functions, *Approx. Theory* **8** (2), 1–11, (1992).
16. Z. Wu, Solving PDE with radial basis function and the error estimation, In *Advances in Computational Mathematics, Lecture Notes on Pure and Applied Mathematics, Volume 202*, (Edited by Z. Chen *et al.*), Guang Zhou, (1998).
17. R. Schaback and C. Franke, Covergence order estimates of meshless collocation methods using radial basis functions, *Advances Computational Mathematics* **8** (4), 381–399, (1998).
18. M.R. Dubal, Domain decomposition and local refinement for multiquadric approximations. I: Second-order equations in one-dimension, *Journal of Applied Science* **1** (1), 146–171, (1994).

19. C.J. Coleman, On the use of radial basis functions in the solution of elliptic boundary value problems, *Computational Mechanics* **17**, 418–422, (1996).
20. M. Sharan, E.J. Kansa and S. Gupta, Application to the multiquadric method for numerical solution of elliptic partial differential equations, *Appl. Math. and Comp.* **84**, 275–302, (1997).
21. Y.C. Hon and X.Z. Mao, An efficient numerical scheme for Burgers' equations, *Appl. Math. and Comp.* **95**, 37–50, (1998).
22. Y.C. Hon, K.F. Cheung and X.Z. Mao, A multiquadric solution for the shallow water equations, *ASCEJ, Hydraulic Engineering* **125** (5), 524–533, (1999).
23. M.R. Dubal, S.R. Olivera and R.A. Matzner, *Approaches to Numerical Relativity*, (Edited by R. d'Inverno), Cambridge University Press, Cambridge, (1993).
24. H. Wendland, Piecewise polynomial, positive definite and compactly supported radial functions of minimal degree, *Adv. Comput. Math.* **4**, 389–396, (1995).
25. R. Schaback and H. Wendland, Using compactly supported radial basis functions to solve partial differential equations, (preprint).
26. A.I. Fedoseyev, M.J. Friedman and E.J. Kansa, Improved multiquadric method for elliptic partial differential equations via PDE collocation on the boundary, (preprint).